
Do current lattice Boltzmann methods for diffusion and advection-diffusion equations respect maximum principles and the non-negative constraint?

AN E-PRINT OF THE PAPER IS AVAILABLE ON ARXIV: 1503.08360

AUTHORED BY

S. KARIMI

Graduate Student, University of Houston.

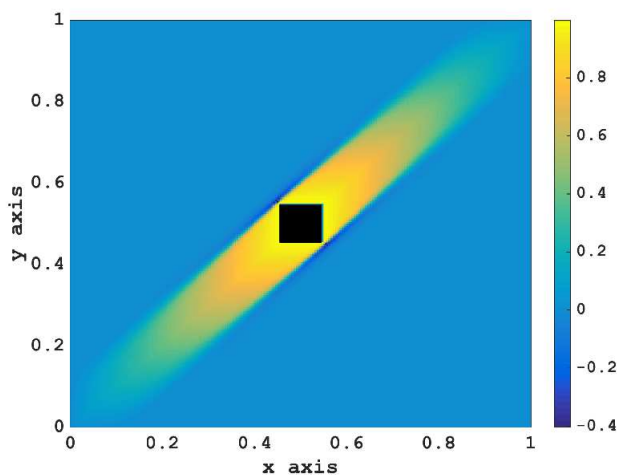
K. B. NAKSHATRALA

Department of Civil & Environmental Engineering

University of Houston, Houston, Texas 77204-4003.

phone: +1-713-743-4418, e-mail: knakshatrala@uh.edu

website: <http://www.cive.uh.edu/faculty/nakshatrala>



This figure shows that a popular multiple-relaxation-time lattice Boltzmann method violates the non-negative constraint for a transient diffusion equation.

2015

COMPUTATIONAL & APPLIED MECHANICS LABORATORY

Do current lattice Boltzmann methods for diffusion and advection-diffusion equations respect maximum principles and the non-negative constraint?

S. Karimi and K. B. Nakshatrala

Department of Civil and Environmental Engineering, University of Houston.

ABSTRACT. The lattice Boltzmann method (LBM) has established itself as a valid numerical method in computational fluid dynamics. Recently, multiple-relaxation-time LBM has been proposed to simulate anisotropic advection-diffusion processes. The governing differential equations of advective-diffusive systems are known to satisfy maximum principles, comparison principles, the non-negative constraint, and the decay property. In this paper, it will be shown that current single- and multiple-relaxation-time lattice Boltzmann methods *fail* to preserve these mathematical properties for transient diffusion and advection-diffusion equations. It will also be shown that the discretization of Dirichlet boundary conditions will affect the performance of lattice Boltzmann methods in meeting these mathematical principles. A new way of discretizing the Dirichlet boundary conditions is also proposed. Several benchmark problems have been solved to illustrate the performance of lattice Boltzmann methods and the effect of discretization of boundary conditions with respect to the aforementioned mathematical properties.

1. INTRODUCTION AND MOTIVATION

The lattice Boltzmann method (LBM) has gained remarkable popularity as a versatile numerical method for fluid dynamics simulations [Chen and Doolen, 1998]. LBM has its roots in the kinetic theory as opposed to the continuum theory. It needs to be emphasized that LBM solves the Boltzmann equation instead of solving the continuum field equations. On the other hand, the finite element method (FEM) and the finite volume method (FVM) solve the continuum field equations directly. Some of the attractive features of LBM are: It can easily handle irregular domains (e.g., unstructured pores and fractures in porous media applications), easy to implement even for complicated flow models, and natural to parallelize [Succi, 2001]. Great advances have been made in extending LBM to simulate multi-phase flows [Falcucci et al., 2006], reactive flows [Rienzo et al., 2012], non-linear chemical reactions [Ayodele et al., 2011], just to name a few. In this paper, we limit our scope to LBM-based formulations for advection-diffusion phenomena.

In the recent years, several key advancements have been made to extend the LBM to simulate transport phenomena. To name a few: [Stiebler et al., 2008], [Shi and Guo, 2009], [Chai and Zhao, 2013], [Yoshida and Nagaoka, 2010] and [Huang and Wu, 2014]. Of these works, Yoshida and

Key words and phrases. lattice Boltzmann method (LBM); meso-scale modeling; multiple-relaxation-time; advection-diffusion equations; comparison principle; maximum principle; non-negative constraint; anisotropy; statistical mechanics.

Nagaoka [Yoshida and Nagaoka, 2010], and Huang and Wu [Huang and Wu, 2014] have proposed multiple-relaxation-time lattice Boltzmann methods to handle advection-diffusion equations with *anisotropic* diffusivity tensors.

The governing equations for a transient advection-diffusion system are parabolic partial differential equations, which possess several important mathematical properties. These properties include the maximum principle and the comparison principle [Protter and Weinberger, 1999; Pao, 1993], which have crucial implications in modeling physical phenomena. For example, a key consequence of the maximum principle in modeling advection-diffusion systems is the non-negative constraint of the attendant chemical species. Several factors such as the physical properties of the medium, topology of the domain, and the spatial and temporal discretization determine the performance of a numerical solution in preserving the *discrete* versions of the mentioned mathematical properties. A discussion on the influence of these factors in the context of the finite element method can be found in [Nakshatrala and Valocchi, 2009]. Violations of these mathematical properties can make a numerical solution inappropriate for scientific and engineering applications. It has been shown that many popular finite element and finite volume formulations for diffusion-type equations violate the maximum principle and the non-negative constraint [Liska and Shashkov, 2008; Nakshatrala and Valocchi, 2009; Nakshatrala et al., 2013b]. Recently, numerical methodologies have been proposed under the finite element method to satisfy the non-negative constraint and the maximum principle by utilizing the underlying variational structure. Since the lattice Boltzmann method does not enjoy such a variational basis, these methodologies developed for the FEM cannot be extended to the lattice Boltzmann method.

To the best of our knowledge, the performance of LBM-based formulations for unsteady diffusion-type equations with respect to comparison principles, maximum principles, and the non-negative constraint has not been documented in the literature. But, such a study is of paramount importance, as LBM-based formulations are being employed in predictive numerical simulations. We shall, therefore, put some popular LBM-based formulations for diffusion-type equations to test, and particularly show that these formulations violate all the aforementioned mathematical principles and physical constraints. The LBM-based formulations of interest in this paper are the non-thermal single-relaxation-time LBM for advection with isotropic diffusion, and the multiple-relaxation-time methods for anisotropic diffusion proposed in [Yoshida and Nagaoka, 2010] and [Huang and Wu, 2014]. The mentioned LBM-based formulations have been chosen merely due to their popularity, and this paper does not pretend to be exhaustive.

The remainder of this paper is organized as follows. Section 2 presents the governing equations for a transient advective-diffusive system along with a brief discussion on the associated mathematical properties. Section 3 reviews the non-thermal single- and multiple-relaxation-time lattice Boltzmann methods for transient diffusion-type equations. In Section 4, several representative test problems are presented with a thorough discussion on the numerical results from LBM-based formulations. Section 5 performs a theoretical analysis on the lattice Boltzmann method to obtain a simple criterion on the time-step and lattice cell size to satisfy the non-negative constraint. Finally, conclusions are drawn in Section 6. On the notational front, a quantity in the continuous setting will be denoted by upright font symbols (e.g., u), and a quantity in the discrete setting will be denoted by italic font (e.g., u).

2. UNSTEADY ANISOTROPIC DIFFUSION-TYPE EQUATIONS

Consider a bounded open domain Ω . We shall denote the boundary of the domain by $\Gamma = \overline{\Omega} - \Omega$, where $\overline{\Omega}$ is the set closure of Ω . We assume that the boundary Γ comprises of two parts Γ^N and Γ^D such that $\Gamma^N \cap \Gamma^D = \emptyset$ and $\Gamma = \Gamma^N \cup \Gamma^D$. We denote the part of the boundary on which Dirichlet boundary condition is prescribed by Γ^D . Neumann boundary condition is prescribed on Γ^N . A spatial point will be denoted by \mathbf{x} . The unit outward normal to the boundary is denoted by $\widehat{\mathbf{n}}(\mathbf{x})$. The time interval of interest will be denoted by $[0, \mathcal{T}]$, and the time is denoted by t . For convenience, we introduce the following differential operator:

$$\mathcal{L}[u(\mathbf{x}, t)] := \frac{\partial u(\mathbf{x}, t)}{\partial t} + \operatorname{div}[\mathbf{v}(\mathbf{x}, t) u(\mathbf{x}, t) - \mathbf{D}(\mathbf{x}) \operatorname{grad}[u(\mathbf{x}, t)]] \quad (2.1)$$

where $u(\mathbf{x}, t)$ is the concentration field. The diffusivity tensor is denoted by $\mathbf{D}(\mathbf{x})$, which is assumed to be symmetric, positive definite, and bounded above. The advection velocity is denoted by $\mathbf{v}(\mathbf{x}, t)$, which is assumed to be solenoidal. That is, $\operatorname{div}[\mathbf{v}] = 0$. The divergence and gradient operators with respect to \mathbf{x} are, respectively, denoted by $\operatorname{div}[\cdot]$ and $\operatorname{grad}[\cdot]$. The initial boundary value problem for a transient advection-diffusion system can be written as follows:

$$\mathcal{L}[u(\mathbf{x}, t)] = g(\mathbf{x}, t) \quad (\mathbf{x}, t) \in \Omega \times (0, \mathcal{T}] \quad (2.2a)$$

$$u(\mathbf{x}, t) = u^P(\mathbf{x}, t) \quad (\mathbf{x}, t) \in \Gamma^D \times [0, \mathcal{T}] \quad (2.2b)$$

$$(\mathbf{v}(\mathbf{x}, t) u(\mathbf{x}, t) - \mathbf{D}(\mathbf{x}) \operatorname{grad}[u(\mathbf{x}, t)]) \cdot \widehat{\mathbf{n}}(\mathbf{x}) = q^P(\mathbf{x}, t) \quad (\mathbf{x}, t) \in \Gamma^N \times [0, \mathcal{T}] \quad (2.2c)$$

$$u(\mathbf{x}, t = 0) = u_0(\mathbf{x}) \quad \mathbf{x} \in \Omega \quad (2.2d)$$

where the source/sink is denoted by $g(\mathbf{x}, t)$, $u^P(\mathbf{x}, t)$ is the prescribed concentration, $q^P(\mathbf{x}, t)$ is the prescribed flux, and the initial concentration is denoted by $u_0(\mathbf{x})$. It is easy to check that equation (2.2a) is a linear parabolic partial differential equation. The initial boundary value problem given by equations (2.2a)–(2.2d) satisfies several important mathematical properties, which will be discussed next.

2.1. Mathematical properties. We introduce the following function space:

$$\mathcal{C}_1^2(\Omega \times (0, \mathcal{T}]) := \left\{ u : \Omega \times [0, \mathcal{T}] \rightarrow \mathbb{R} \mid u, \frac{\partial u}{\partial t}, \frac{\partial u}{\partial x_i}, \frac{\partial^2 u}{\partial x_i \partial x_j} \in \mathcal{C}(\Omega \times (0, \mathcal{T}]) \right\} \quad (2.3)$$

where $\mathcal{C}(\Omega \times (0, \mathcal{T}])$ is the set of all continuous functions defined on $\Omega \times (0, \mathcal{T}]$. Similarly, one can define $\mathcal{C}(\overline{\Omega} \times [0, \mathcal{T}])$.

PROPERTY 1 (The maximum principle). *Let $u(\mathbf{x}, t) \in \mathcal{C}_1^2(\Omega \times (0, \mathcal{T}]) \cap \mathcal{C}(\overline{\Omega} \times [0, \mathcal{T}])$ be a solution of the initial boundary value problem (2.2) with $\partial\Omega = \Gamma^D$. If $g(\mathbf{x}, t) \geq 0$ then*

$$\min_{(\mathbf{x}, t) \in \overline{\Omega} \times [0, \mathcal{T}]} u(\mathbf{x}, t) = \min \left[\min_{(\mathbf{x}, t) \in \Gamma \times [0, \mathcal{T}]} u(\mathbf{x}, t), \min_{\mathbf{x} \in \Omega} u_0(\mathbf{x}) \right] \quad (2.4)$$

PROPERTY 2 (The comparison principle). *Let $u_1(\mathbf{x}, t)$ and $u_2(\mathbf{x}, t)$ belong to $\mathcal{C}_1^2(\Omega \times (0, \mathcal{T}]) \cap \mathcal{C}(\overline{\Omega} \times [0, \mathcal{T}])$. If $\mathcal{L}[u_1(\mathbf{x}, t)] \geq \mathcal{L}[u_2(\mathbf{x}, t)]$ on $\Omega \times (0, \mathcal{T}]$, and $u_1^P(\mathbf{x}, t) \geq u_2^P(\mathbf{x}, t)$ on $\Gamma \times [0, \mathcal{T}]$ then $u_1(\mathbf{x}, t) \geq u_2(\mathbf{x}, t)$ on $\overline{\Omega} \times [0, \mathcal{T}]$.*

Mathematical proofs to the maximum principle and the comparison principle can found in [Evans, 1998]. We now show that the non-negative constraint for the concentration can be obtained as a consequence of the maximum principle under certain assumptions on the input data. One could

alternatively obtain the non-negative constraint from the comparison principle, which we would not present here.

PROPERTY 3 (The non-negative constraint). *If $g(\mathbf{x}, t) \geq 0$ in Ω , $u^p(\mathbf{x}, t) \geq 0$ on Γ , and $u_0(\mathbf{x}) \geq 0$ in Ω then*

$$u(\mathbf{x}, t) \geq 0 \quad \text{in } \overline{\Omega} \text{ and } \forall t \quad (2.5)$$

PROOF. Based on the hypothesis, we have the following two results:

$$\min_{(\mathbf{x}, t) \in \Gamma \times [0, T]} u(\mathbf{x}, t) = \min_{(\mathbf{x}, t) \in \Gamma \times [0, T]} u^p(\mathbf{x}, t) \geq 0 \quad (2.6)$$

$$\min_{\mathbf{x} \in \Omega} u_0(\mathbf{x}) \geq 0 \quad (2.7)$$

These further imply that

$$\min \left[\min_{(\mathbf{x}, t) \in \Gamma \times [0, T]} u(\mathbf{x}, t), \min_{\mathbf{x} \in \Omega} u_0(\mathbf{x}) \right] \geq 0 \quad (2.8)$$

From the maximum principle, we can conclude that

$$\min_{(\mathbf{x}, t) \in \overline{\Omega} \times [0, T]} u(\mathbf{x}, t) \geq 0 \quad (2.9)$$

which gives the desired result that $u(\mathbf{x}, t) \geq 0$ in $\overline{\Omega}$ and $\forall t$. \square

The following integrals will be used in the remainder of this paper:

$$\begin{aligned} \mathcal{J}_1(u; \Omega; t) &:= \int_{\Omega} u(\mathbf{x}, t) \, d\Omega, & \mathcal{J}_1^+(u; \Omega; t) &:= \int_{\Omega} \max[u(\mathbf{x}, t), 0] \, d\Omega, \\ \mathcal{J}_2(u; \Omega; t) &:= \int_{\Omega} u^2(\mathbf{x}, t) \, d\Omega, & \mathcal{J}_2^+(u; \Omega; t) &:= \int_{\Omega} (\max[u(\mathbf{x}, t), 0])^2 \, d\Omega \end{aligned} \quad (2.10)$$

PROPERTY 4 (The decay property). *If $\mathbf{v}(\mathbf{x}, t) = \mathbf{0}$, $u^p(\mathbf{x}, t) = 0$ on the entire Γ , and $g(\mathbf{x}, t) = 0$ in Ω then*

$$\frac{d}{dt} \mathcal{J}_2(u; \Omega; t) \leq 0 \quad \forall t \quad (2.11)$$

PROOF. Noting that $g(\mathbf{x}, t) = 0$ and $\mathbf{v}(\mathbf{x}, t) = \mathbf{0}$, equation (2.2a) implies the following:

$$\int_{\Omega} u \frac{\partial u}{\partial t} \, d\Omega - \int_{\Omega} u \operatorname{div}[\mathbf{D}(\mathbf{x}) \operatorname{grad}[u]] \, d\Omega = 0 \quad (2.12)$$

Using Green's identity and noting that $u(\mathbf{x}, t) = u^p(\mathbf{x}, t) = 0$ on Γ , we obtain the following:

$$\int_{\Omega} u \frac{\partial u}{\partial t} \, d\Omega + \int_{\Omega} \operatorname{grad}[u] \cdot \mathbf{D}(\mathbf{x}) \operatorname{grad}[u] \, d\Omega = 0 \quad (2.13)$$

Noting that $\mathbf{D}(\mathbf{x})$ is a positive definite second-order tensor, we have:

$$\int_{\Omega} u \frac{\partial u}{\partial t} \, d\Omega \leq 0 \quad (2.14)$$

This further implies that

$$\frac{d}{dt} \int_{\Omega} u^2(\mathbf{x}, t) \, d\Omega \equiv \frac{d}{dt} \mathcal{J}_2(u; \Omega; t) \leq 0 \quad (2.15)$$

In order to obtain the above result, we have assumed that Ω is independent of t , which is the case in this paper. \square

In the subsequent sections we will illustrate the performance of some popular LBM-based formulations with respect to the aforementioned mathematical properties in the discrete setting. We will also compare the performance of the lattice Boltzmann method with the finite element method in this regard.

3. THE LATTICE BOLTZMANN METHOD

The lattice Boltzmann method is a numerical method for solving the Boltzmann equation. A numerical simulation based on LBM will provide an approximate distribution of particles in the discrete configuration-momentum space. Macroscopic quantities such as concentration can then be calculated using the obtained discrete distributions. In this paper, we will consider the Bhatnagar-Gross-Krook (BGK) model for the collision term:

$$\frac{\partial f}{\partial t} + \frac{1}{m} \mathbf{p} \cdot \text{grad} [f] + \mathbf{F} \cdot \frac{\partial f}{\partial \mathbf{p}} = \frac{1}{\lambda} (f^{\text{eq}} - f) \quad (3.1)$$

where the continuous distribution function is denoted by $f = f(\mathbf{p}, \mathbf{x}, t)$, the equilibrium distribution is denoted by f^{eq} , λ is the relaxation time, the macroscopic momentum is denoted by \mathbf{p} , and \mathbf{F} is the external force. We shall use the symbol τ for the non-dimensional relaxation time. We will now specialize on the LBM-based formulations for isotropic and anisotropic advection-diffusion equations. However, for an in-depth discussion on the lattice Boltzmann method, one can consult the references [He and Lou, 1997; Succi, 2001]. We first present the single-relaxation-time lattice Boltzmann method, and then followed by multiple-relaxation-time methods.

3.1. The single-relaxation-time lattice Boltzmann method. We will use a uniform and structured discretization of the spatial domain Ω . The lattice cell size is denoted by Δx , and Δt is the time-step. We will consider a $DnQm$ lattice model, where n is the number of spatial dimensions and m is the number of discretized directions for momentum. The lattice models that are employed in this paper are shown in Figure 1. The distribution of particles at a lattice node \mathbf{x} , at time t and along the velocity direction \mathbf{e}_i will be denoted by $f_i(\mathbf{x}, t)$. The evolution of the discretized distributions is governed by the following formula:

$$f_i(\mathbf{x} + \mathbf{e}_i \Delta t, t + \Delta t) = \widehat{f}_i(\mathbf{x}, t) \quad [\text{translation step}] \quad (3.2)$$

where the post-collision distribution is denoted by \widehat{f}_i and is defined as follows:

$$\widehat{f}_i(\mathbf{x}, t) = f_i(\mathbf{x}, t) - \frac{1}{\tau} (f_i(\mathbf{x}, t) - f_i^{\text{eq}}(\mathbf{x}, t)) + w_i \Delta t g(\mathbf{x}, t) \quad [\text{collision step}] \quad (3.3)$$

where $g(\mathbf{x}, t)$ is the source/sink at a lattice node. The weight associated with the i -th velocity direction is denoted by w_i . The equilibrium distribution for the i -th velocity direction will be denoted by f_i^{eq} . A popular choice for the equilibrium distribution of an advective-diffusive system takes the following form:

$$f_i^{\text{eq}}(\mathbf{x}, t) = w_i u(\mathbf{x}, t) \left(1 + \frac{\mathbf{v}(\mathbf{x}, t) \cdot \mathbf{e}_i}{c_s^2} \right) \quad (3.4)$$

where advection velocity is denoted by \mathbf{v} , and c_s is the lattice (sound) velocity. The relaxation time is given by the following relation:

$$\tau = \frac{D}{\Delta t c_s^2} + \frac{1}{2} \quad (3.5)$$

where D is the (isotropic) diffusion coefficient. The concentration at a lattice node can then be calculated as:

$$u(\mathbf{x}, t) = \sum_{i=1}^m f_i(\mathbf{x}, t) \quad (3.6)$$

We now describe the discretization of boundary conditions.

- (i) *Standard method for Dirichlet boundary conditions:* Let $\{j\}$ be the set of unknown distributions at a point $\mathbf{x} \in \Gamma^D$, and $\{i\}$ the set of known distributions at that point. We can then write

$$f_\alpha(\mathbf{x}, t) = \frac{w_\alpha}{\sum_{p \in \{j\}} w_p} \left(u^p(\mathbf{x}, t) - \sum_{q \in \{i\}} f_q(\mathbf{x}, t) \right) \quad \forall \alpha \in \{j\} \quad (3.7)$$

It will be shown that this standard way of discretizing Dirichlet boundary conditions can contribute to the violation of the non-negative constraint. We, therefore, propose a new way of discretizing the Dirichlet boundary conditions.

- (ii) *Weighted splitting method for Dirichlet boundary conditions:* Let \mathbf{x} be the spatial coordinates of a lattice node on Γ^D . The discretized distributions at each time-level will be assigned as follows:

$$f_\alpha(\mathbf{x}, t) = w_\alpha u^p(\mathbf{x}, t) \quad \alpha = 0, \dots, m-1 \quad (3.8)$$

where u^p is the prescribed concentration.

- (iii) *Neumann boundary conditions:* Let $\{j\}$ be the set of unknown distributions at a point $\mathbf{x} \in \Gamma^N$. We can then discrete the Neumann boundary conditions as follows:

$$f_\alpha(\mathbf{x}, t + \Delta t) = \widehat{f}_\beta(\mathbf{x}, t) + \frac{1}{c_s} q^p(\mathbf{x}, t + \Delta t) \frac{\mathbf{e}_\alpha \cdot \widehat{\mathbf{n}}(\mathbf{x})}{\sum_{k \in j} \mathbf{e}_k \cdot \widehat{\mathbf{n}}(\mathbf{x})} \quad \forall \alpha \in \{j\} \quad (3.9)$$

where β is the index of a discrete velocity direction such that $\mathbf{e}_\alpha = -\mathbf{e}_\beta$, and q^p is the prescribed flux. Note that $\mathbf{e}_\alpha \cdot \widehat{\mathbf{n}}(\mathbf{x}) < 0$ for $\alpha \in \{j\}$.

3.2. The multiple-relaxation-time lattice Boltzmann methods. The single-relaxation-time lattice Boltzmann methods are limited to isotropic diffusion. Multiple-relaxation-time lattice Boltzmann methods offer a more suitable framework for simulating anisotropic diffusion, and are more easily presentable in the momentum space [Lallemand and Lou, 2000; Li et al., 2010]. The distributions can be transformed to moments using the following linear operation:

$$|\varrho_i\rangle(\mathbf{x}, t) = \mathbf{M} |f_i\rangle(\mathbf{x}, t) \quad (3.10)$$

where \mathbf{M} is an $m \times m$ orthogonal transformation matrix, and $|f_i\rangle(\mathbf{x}, t)$ is the column vector of size $m \times 1$ of the distributions at lattice node \mathbf{x} and at time t . The moment corresponding to f_i is denoted by ϱ_i . The BGK lattice Boltzmann equation can then be written as follows:

$$|\varrho_i\rangle(\mathbf{x} + \mathbf{e}_i \Delta t, t + \Delta t) = |\varrho_i\rangle(\mathbf{x}, t) - \mathbf{S} \left(|\varrho_i\rangle(\mathbf{x}, t) - |\varrho_i^{\text{eq}}\rangle(\mathbf{x}, t) \right) + \Delta t \mathbf{M} |w_i\rangle g(\mathbf{x}, t) \quad (3.11)$$

where \mathbf{S} is the $m \times m$ matrix of relaxation times. In the case of the single-relaxation-time lattice Boltzmann method, the matrix \mathbf{S} will be $\mathbf{S} = \mathbf{I}_m / \tau$, where \mathbf{I}_m is the $m \times m$ identity matrix, and τ is defined in equation (3.5). The matrix \mathbf{S} need not remain diagonal in the case of anisotropic diffusion. In this paper, we shall use the multiple-relaxation-time methods proposed in [Yoshida and Nagaoka, 2010; Huang and Wu, 2014]. The treatment of boundary conditions will remain unchanged to what was presented earlier (i.e., equations (3.7)–(3.9)).

4. REPRESENTATIVE NUMERICAL RESULTS

In this section, we employ the single- and multiple-relaxation-time lattice Boltzmann methods to solve representative diffusion and advection-diffusion problems. For brevity, we shall refer to the multiple-relaxation-time method proposed in [Yoshida and Nagaoka, 2010] as the Y-N method, and to the multiple-relaxation-time method proposed in [Huang and Wu, 2014] as the H-W method. In all the numerical simulations that employ the H-W method, we have taken $c_1 = 1$, $c_2 = -2$, $\alpha_1 = 8$, $\alpha_2 = -8$ and $s_0 = s_1 = \dots = s_m = 1$ (cf., equations (15)–(17) in [Huang and Wu, 2014]). In the rest of this section, we shall use the following notation:

$$u_{\min}(t) = \min_{\mathbf{x} \in \Omega} u(\mathbf{x}, t) \quad (4.1)$$

$$u_{\max}(t) = \max_{\mathbf{x} \in \Omega} u(\mathbf{x}, t) \quad (4.2)$$

In all the problems that follow, the distributions f_i are initialized as follows:

$$f_i(\mathbf{x}, t = 0) = w_i u_0(\mathbf{x}) \quad (4.3)$$

4.1. One-dimensional problems. Consider the computational domain to be $\Omega = (0, 1)$. The diffusion coefficient is taken as $D = 1/3$, and the advection is neglected. The governing equations take the following form:

$$\frac{\partial u(\mathbf{x}, t)}{\partial t} - \text{div} [D \text{grad} [u(\mathbf{x}, t)]] = g(\mathbf{x}, t) \quad (\mathbf{x}, t) \in \Omega \times (0, \mathcal{T}] \quad (4.4a)$$

$$u(\mathbf{x}, t) = u^P(\mathbf{x}, t) \quad (\mathbf{x}, t) \in \Gamma^D \times [0, \mathcal{T}] \quad (4.4b)$$

$$-\hat{\mathbf{n}} \cdot D \text{grad} [u] = q^P(\mathbf{x}, t) \quad (\mathbf{x}, t) \in \Gamma^N \times [0, \mathcal{T}] \quad (4.4c)$$

$$u(\mathbf{x}, t = 0) = u_0(\mathbf{x}) \quad \mathbf{x} \in \bar{\Omega} \quad (4.4d)$$

We employ the *D1Q3* lattice model with weights $w_1 = 1/2$, and $w_2 = w_3 = 1/4$. Several different cases are considered below.

4.1.1. *Uniform initial conditions.* Consider the following initial and boundary conditions:

$$u_0(\mathbf{x}, t = 0) = 1 \quad \forall \mathbf{x} \in \Omega \quad (4.5a)$$

$$q^P(x = 0, t) = 0 \quad (4.5b)$$

$$u^P(x = 1, t) = 0 \quad (4.5c)$$

where $t \in [0, 10^{-2}]$. According to the maximum principle, the concentration should remain in $[0, 1]$ at all times. The following conclusions can be drawn from Figures 2 and 3:

- (a) The single-relaxation-time lattice Boltzmann method for diffusion equations violates the maximum principle. Although the minimum observed nodal concentration is zero, some of the nodal concentrations exceeded unity.
- (b) For a given time-step, the violation of the maximum principle can be reduced by reducing the lattice cell size Δx . As we will see later, this need not be the case when the diffusion is anisotropic.

4.1.2. *Non-uniform initial conditions.* Consider the following initial condition:

$$u_0(\mathbf{x}, t = 0) = \begin{cases} 1 & \mathbf{x} \in [0.4, 0.6] \\ 0 & \text{otherwise} \end{cases} \quad (4.6)$$

TABLE 1. One-dimensional problem with uniform initial condition and constant source: This table compares the numerical solutions under the standard and weighted splitting methods for discretizing Dirichlet boundary conditions for several choices of Δx and Δt . In this numerical experiment, one observes that the weighted splitting method produces non-negative solutions, and Its accuracy is comparable to the standard method of discretization.

Δt	Δx	$1/\tau$	standard method		weighted splitting method	
			violation	Error(\mathcal{T})	violation	Error(\mathcal{T})
10^{-3}	10^{-3}	9.995×10^{-4}	Yes	3.14×10^{-4}	No	3.15×10^{-4}
10^{-4}	10^{-3}	1.000×10^{-1}	Yes	2.98×10^{-4}	No	3.10×10^{-4}
10^{-5}	10^{-3}	9.520×10^{-2}	Yes	2.90×10^{-4}	No	2.94×10^{-4}
10^{-6}	10^{-3}	6.667×10^{-1}	Yes	2.90×10^{-4}	No	2.90×10^{-4}
10^{-7}	10^{-3}	1.667×10^0	Yes	2.90×10^{-4}	No	2.90×10^{-4}

The boundary conditions are:

$$u^P(x=1, t) = 0 \quad (4.7a)$$

$$q^P(x=0, t) = 0 \quad (4.7b)$$

Even for this problem, the concentration should remain in $[0, 1]$. Maximum and minimum nodal concentrations ($u_{\min}(t)$ and $u_{\max}(t)$) are shown in Figures 4 and 5. The following conclusions can be made from these figures:

- (a) The maximum and minimum bounds can be violated simultaneously.
- (b) Decreasing the time-step while keeping the lattice cell size constant will not alleviate the violations of the non-negative constraint and the maximum principle.
- (c) Just like the previous problem, the violations vanish with the refinement of the lattice cell size for a fixed time-step.

4.1.3. *Uniform initial condition with constant source.* We have taken $u_0(x) = 0$ on the entire domain $\Omega = (0, 1)$, and $\Gamma^D = \Gamma$ with $u^P(x \in \Gamma, t) = 0$. The time interval of interest is taken as $\mathcal{T} = 10^{-2}$. The source is taken as $g(x, t) = 1$ for $x \in \Omega$ and $t \in (0, \mathcal{T}]$. The error will be calculated as follows:

$$\text{Error}(t) = \frac{1}{N} \sqrt{\sum_{i=1}^N (u(x_i, t) - u_{\text{exact}}(x_i, t))^2} \quad (4.8)$$

where N is the total number of lattice nodes, and x_i is the spatial coordinate of the i -th lattice node. The exact solution to this problem is denoted by $u_{\text{exact}}(x, t)$. *The obtained numerical results are summarized in Table 1, and one can conclude that the weighted splitting method for discretizing the Dirichlet boundary conditions produces non-negative nodal concentrations for one-dimensional problems. However, the method comes at an expense of marginal decrease in accuracy.*

4.1.4. *On comparison principle.* Consider the following boundary and initial conditions:

$$u_0(x, t=0) = 0 \quad x \in \Omega \quad (4.9a)$$

$$u^P(x=0, t) = u_L \quad t \in [0, \mathcal{T}] \quad (4.9b)$$

$$u^P(x=1, t) = 0 \quad t \in [0, \mathcal{T}] \quad (4.9c)$$

In this numerical experiment, we have taken $\mathcal{T} = 0.01$, and the source term is taken to be zero (i.e., $g(\mathbf{x}, t) = 0$). We shall solve the problem using several cases of Δx , Δt , and u_L . Both the standard and weighted splitting methods are employed in separate test runs.

For this problem, if $u_L^1 \leq u_L^2$ then the comparison principle implies that $u^1(\mathbf{x}, t) \leq u^2(\mathbf{x}, t)$ for $\forall (\mathbf{x}, t) \in \overline{\Omega} \times [0, \mathcal{T}]$. A sample result is presented in Figure 6. Several other numerical experiments are performed using different choices of Δx and Δt . Figure 6 and these numerical experiments reveal the following conclusions:

- (a) LBM-based formulations do not, in general, respect the comparison principle.
- (b) For one-dimensional problems, refining the lattice cell size Δx for a given time-step Δt can remove the violations of the comparison principle.
- (c) The weighted splitting method does not guarantee the satisfaction of the comparison principle even in 1D.

4.2. Two-dimensional problem with anisotropic diffusion on a non-convex domain.

We now examine the Y-N multiple-relaxation-time method for anisotropic diffusion tensor. The computational domain is shown in Figure 7. We have taken $L = 1$ and $\Gamma^D = \Gamma_{\text{outer}} \cup \Gamma_{\text{inner}}$. On the inner boundary the prescribed concentration is prescribed to be unity (i.e., $u^P(\mathbf{x}, t) = 1$ for $\mathbf{x} \in \Gamma_{\text{inner}}$). The flux is prescribed to be zero on the outer boundary (i.e., $q^P(\mathbf{x}, t) = 0$ for $\mathbf{x} \in \Gamma_{\text{outer}}$). The anisotropic diffusion tensor is taken as:

$$\mathbf{D}(\mathbf{x}) = \mathbf{R}_\theta^T \mathbf{D}_0 \mathbf{R}_\theta \quad (4.10)$$

where

$$\mathbf{D}_0 = \begin{bmatrix} 10 & 0 \\ 0 & 10^{-3} \end{bmatrix} \quad (4.11)$$

The orthogonal rotation matrix is denoted by \mathbf{R}_θ , where θ denotes the angle of rotation. Herein, we have taken $\theta = \pi/4$. We employed the $D2Q5$ lattice model. The discrete velocity directions are given by

$$\mathbf{e}_i^T = \begin{cases} [0, 0] & i = 0 \\ c[\cos((i-1)\pi), \sin((i-1)\pi)] & i = 1, 2 \\ c[\cos((2i-5)\pi/2), \sin((2i-5)\pi/2)] & i = 3, 4 \end{cases} \quad (4.12)$$

where $c = \Delta x / \Delta t$. The respective weights are taken as:

$$w_i = \begin{cases} 1/3 & i = 0 \\ 1/6 & i = 1, 2, 3, 4 \end{cases} \quad (4.13)$$

The time interval of interest is taken as $\mathcal{T} = 10^{-2}$. We employed the standard method of enforcing Dirichlet boundary conditions (see equation (3.7)). Table 2 provides the discretization parameters employed in this paper. Figures 8–10 show that the Y-N method violates the non-negative constraint. In fact, the obtained minimum concentration is about -0.4 , which is a significant violation given the fact that the concentration should be between 0 and 1. Another noticeable feature in all the cases considered, the minimum concentration converged to a negative value as the time progressed.

TABLE 2. Two-dimensional problem with anisotropic diffusion tensor on a non-convex domain: This table provides the minimum concentrations for various discretization parameters (i.e., Δx and Δt). We have taken $\Delta x^2 = \Delta t$.

Case	Δx	Δt	$u_{\min}(\mathcal{T})$
1	1.25×10^{-2}	1.5625×10^{-4}	-0.3781
2	1.00×10^{-2}	1.0000×10^{-4}	-0.4072
3	5.00×10^{-3}	2.5000×10^{-5}	-0.4044

4.3. Two-dimensional problem with anisotropic and heterogeneous diffusion tensor.

Consider the spatial domain to be $\Omega = (0, 1) \times (0, 1)$. We have taken the following anisotropic and heterogeneous diffusivity tensor:

$$\mathbf{D}(x, y) = \epsilon' \mathbf{I}_2 + \begin{bmatrix} \epsilon x^2 + y^2 & -(1 - \epsilon)xy \\ -(1 - \epsilon)xy & x^2 + \epsilon y^2 \end{bmatrix} \quad (4.14)$$

where $\epsilon \ll 1$ and $\epsilon' \ll 1$ are arbitrary constants, and \mathbf{I}_2 denotes the 2×2 identity matrix. For this numerical experiment, we have taken $\epsilon = 10^{-3}$ and $\epsilon' = 10^{-10}$. The prescribed concentration on the entire boundary is taken to be zero. The initial concentration is taken as:

$$u_0(x, y) = \begin{cases} 1 & (x, y) \in [0.4, 0.6] \times [0.4, 0.6] \\ 0 & \text{otherwise} \end{cases} \quad (4.15)$$

The time interval of interest is taken as $\mathcal{T} = 0.025$. The H-W method based on the $D2Q9$ lattice model is employed with the lattice velocity $c = \Delta x / \Delta t$. The discrete momenta are taken as:

$$\mathbf{e}_i^T = \begin{cases} [0, 0] & i = 0 \\ c [\cos((i-1)\pi/2), \sin((i-1)\pi/2)] & i = 1, 2, 3, 4 \\ \sqrt{2}c [\cos((2i-9)\pi/4), \sin((2i-9)\pi/4)] & i = 5, 6, 7, 8 \end{cases} \quad (4.16)$$

with the following weights:

$$w_i = \begin{cases} 4/9 & i = 0 \\ 1/9 & i = 1, 2, 3, 4 \\ 1/36 & i = 5, 6, 7, 8 \end{cases} \quad (4.17)$$

The problem is solved using different choices of Δx and Δt , which are provided in Table 3. This table also provides insight on the performance of the H-W method. The spread of the lattice nodes that experience violation of non-negative constraint is shown in Figures 11 and 12. The following conclusions can be drawn from Figures 11–14 and Table 3:

- (a) The H-W multiple-relaxation-time method violates the non-negative constraint when the diffusion is anisotropic.
- (b) As discussed earlier, the integral \mathcal{J}_2 should decrease monotonically with time for pure diffusion equations. However, the H-W method does not respect the decay property. Clipping procedure can eliminate the violation of the non-negative constraint but does not eliminate the violation of the decay property. However, it has been observed that refining the discretization parameters (i.e., Δx and Δt) can improve the performance of numerical solutions with respect to the decay property.
- (c) In the case of the integral \mathcal{J}_1 , noticeable differences appear between the numerical solution with negative values and the numerical solution with the negative values clipped.

TABLE 3. Two-dimensional problem with anisotropic and heterogeneous diffusion tensor: In this table, the number of nodes that experience violations of the non-negative constraint N_{neg} , the minimum and maximum observed concentration for various choices of Δx and Δt are shown

Note that in all the cases, despite refining the lattice cell size, the non-negative constraint is violated. The number of nodes that have negative values for the concentration is denoted by

N_{neg} . The total number of lattice nodes is denoted by N .

Case	Δx	Δt	$N_{\text{neg}}/N \times 100$	$u_{\min}(\mathcal{T})$	$u_{\max}(\mathcal{T})$
1	5.00×10^{-2}	1.00×10^{-3}	$90/441 \times 100 = 20.41\%$	-0.0472	0.5379
2	2.50×10^{-2}	2.50×10^{-4}	$762/1681 \times 100 = 45.33\%$	-0.0311	0.5576
3	1.25×10^{-2}	6.25×10^{-5}	$2867/6561 \times 100 = 43.70\%$	-0.0193	0.5768
4	1.00×10^{-2}	4.00×10^{-5}	$4207/10201 \times 100 = 41.24\%$	-0.0144	0.6188
5	5.00×10^{-3}	1.00×10^{-5}	$11894/40401 \times 100 = 29.44\%$	-0.0068	0.6021

4.4. Fast bimolecular reaction. Consider a simple chemical reaction of the form:



where A , B and C are the participating chemical species; and n_A , n_B and n_C are their respective stoichiometry coefficients. We are interested in the fate of the product C when the time-scale of the chemical reaction is much faster than that of the transport processes (i.e., diffusion and advection). A detailed description of this mathematical model can be found in [Nakshatrala et al., 2013a], and will not be repeated here. However, the mentioned paper neglected advection in all their numerical examples, and the entire paper is devoted to the finite element method.

4.4.1. *Fast bimolecular reaction in a porous medium.* We consider the combined effect of transport and chemical reactions in a porous medium. Problems of this type are frequently encountered in precipitation studies and ground-water hydrology [Willingham et al., 2008]. It needs to be mentioned that Willingham *et al.* [Willingham et al., 2008] have performed numerical modeling but employed the finite volume method for the transport problem and LBM for the flow problem. We will investigate whether the non-negative constraint will be violated in the numerical simulations of such situations under LBM for both flow and transport problems. In the first numerical experiment, we shall assume the diffusivity tensor to be isotropic. The advection velocity will be determined by solving the incompressible Navier-Stokes equations in the pore structure (see Figure 15). That is, obtain $\mathbf{v}(\mathbf{x}, t)$ and $p(\mathbf{x}, t)$ by solving:

$$\rho \left(\frac{\partial \mathbf{v}}{\partial t} + \mathbf{v} \cdot \text{grad} [\mathbf{v}] \right) = -\text{grad} [p] + \mu \text{div} \left[\text{grad} [\mathbf{v}] + \text{grad} [\mathbf{v}]^T \right] \quad (4.19a)$$

$$\text{div} [\mathbf{v}] = 0 \quad (4.19b)$$

where $\mathbf{v} = \mathbf{v}(\mathbf{x}, t)$ is the velocity, $p = p(\mathbf{x}, t)$ is the pressure, ρ is the density of the fluid, and μ is the coefficient of viscosity. The density is taken as $\rho = 1$, and the viscosity of the fluid is taken to be $\mu = 10^{-2}$. The components of the inlet velocity are $v_x^{\text{inlet}} = 1$ and $v_y^{\text{inlet}} = 0$. Diffusion coefficient of all the chemical species is taken as $D = 10^{-2}$. A pictorial description of the problem is given in Figure 15. The prescribed concentrations for the chemical species A and B are $u_A^p = 1$ and $u_B^p = 1$. The stoichiometry coefficients are taken as $n_A = 1$, $n_B = 2$, and $n_C = 1$. The dimensions of the computational domain are $L_x = 1/2$ and $L_y = 2$. The time interval of interest is taken as $\mathcal{T} = 0.5$.

TABLE 4. Fast bimolecular reaction in a porous medium: Discretization parameters used in the numerical experiment.

Case	Δx	Δt
1	6.25×10^{-3}	9.75×10^{-4}
2	5.00×10^{-3}	6.25×10^{-4}

Table 4 provides the choices of Δx and Δt employed in the numerical simulation. We employed the single-relaxation-time lattice Boltzmann method using the $D2Q9$ lattice model for both flow and transport problems (i.e., see equation (4.16)). The concentration of the chemical species A , B and C are shown in Figures 16–17. No negative values for the concentration are observed for the reactants A and B , which is the result of equations (3.6a) and (3.6b) in [Nakshatrala et al., 2013a]. However, the concentration of the product C exhibited negative values, which is shown in Figure 18. These negative values are very small in comparison with the maximum concentration in the domain. We also observed that refining the discretization parameters, Δt and Δx , can reduce the violation of the non-negative constraint, unlike the previous problems with anisotropic diffusion tensor.

4.4.2. *Fast bimolecular reaction in an anisotropic and heterogeneous medium.* We will consider the domain given in Figure 19. Dimensions of the domain are $L_x = 2$ and $L_y = 1$. The advection velocity will be derived from the following stream function:

$$\psi(x, y) = -y - \sum_{k=1}^3 \alpha_k \cos\left(\frac{p_k \pi x}{L_x} - \frac{\pi}{2}\right) \sin\left(\frac{q_k \pi y}{L_y}\right) \quad (4.20)$$

where the parameters are given by

$$(p_1, p_2, p_3) = (4.0, 5.0, 10.0), \quad (q_1, q_2, q_3) = (1.0, 5.0, 10.0), \quad (\alpha_1, \alpha_2, \alpha_3) = (0.08, 0.02, 0.01) \quad (4.21)$$

The components of the advection velocity are calculated as:

$$v_x(x, y) = -\frac{\partial \psi(x, y)}{\partial y}, \quad v_y(x, y) = +\frac{\partial \psi(x, y)}{\partial x} \quad (4.22)$$

The dispersion tensor is taken as:

$$\mathbf{D}(x, y) = 10^{-5} \mathbf{I} + \beta_T \|\mathbf{v}\| \mathbf{I} + (\beta_L - \beta_T) \frac{\mathbf{v} \otimes \mathbf{v}}{\|\mathbf{v}\|} \quad (4.23)$$

where \otimes denotes the tensor product, \mathbf{I} is the 2×2 identity tensor, $\|\cdot\|$ is the 2-norm, $\beta_T = 10^{-4}$, and $\beta_L = 1$. The prescribed concentrations are $u_A^p = u_B^p = 1$, and the stoichiometry coefficients are $n_A = 1$, $n_B = 2$ and $n_C = 1$. The time interval of interest is $\mathcal{T} = 0.25$. We employed the $D2Q9$ lattice model using the H-W method, and obtained the numerical solution for the fate of the product C . Discretization parameters for various cases are given in Table 5. *Figures 20–22 clearly show that the H-W method violated the non-negative constraint, and the violations did not vanish either with time or with refinement of the discretization parameters.*

5. A THEORETICAL ANALYSIS

In this section, we will provide a simple criterion in terms of the discretization parameters to satisfy the non-negative constraint for one-dimensional problems. We will also limit our scope to

TABLE 5. Fast bimolecular reaction in anisotropic and heterogeneous medium: Different discretization parameters and violation of the non-negative constraint.

Case	Δx	Δt	$u_{\min}(\mathcal{T})$	$u_{\max}(\mathcal{T})$	$N_{\text{neg}}/N \times 100$
1	5.00×10^{-2}	2.50×10^{-4}	-0.0209	0.2704	$275/861 \times 100 = 31.94\%$
2	2.50×10^{-2}	6.25×10^{-5}	-0.0394	0.3072	$1283/3321 \times 100 = 38.63\%$
3	1.25×10^{-2}	1.56×10^{-6}	-0.0481	0.3136	$5703/13041 \times 100 = 43.73\%$

pure diffusion equations (i.e., $\mathbf{v}(\mathbf{x}, t) = \mathbf{0}$), and $\partial\Omega = \Gamma^D$. We will restrict the analysis to the *D1Q3* lattice model. We initialize the discrete distributions f_i at all lattice nodes as follows:

$$f_i(x, t = 0) = w_i u_0(x) \quad (5.1)$$

Since $w_i > 0$ and $u_0(x) \geq 0$, we have $f_i(x, 0) \geq 0$. Furthermore, we assume that the Dirichlet boundary conditions will be discretized using the *weighted splitting method* (see equation (3.8)). The weighted splitting method guarantees the non-negativity of distributions f_i for a lattice node on the boundary provided that the prescribed concentration on Γ^D is non-negative. That is,

$$\text{if } u^p(x \in \Gamma^D, t) \geq 0 \text{ then } f_i(x \in \Gamma^D, t) \geq 0 \quad (5.2)$$

So far, we made sure that all the distributions at the previous time-level are non-negative, and the discretization of the boundary conditions will not disrupt the non-negativity of distributions. Since the distributions at time t are non-negative, equilibrium distributions f_i^{eq} will be non-negative in the calculation of the collision step at time $t + \Delta t$. That is,

$$f_i(x, t) \geq 0 \Rightarrow u(\mathbf{x}, t) = \sum_i f_i(x, t) \geq 0 \Rightarrow f_i^{\text{eq}}(\mathbf{x}, t) = w_i u(\mathbf{x}, t) \geq 0 \quad (5.3)$$

If all of these conditions are satisfied, restricting the value of the relaxation time τ in equation (3.3) can lead to non-negative concentrations at all lattice nodes and for all time-levels. We require that

$$1 - 1/\tau \geq 0 \quad (5.4)$$

Using equation (3.5) and the above inequality, one can obtain the following condition that ensures non-negativity:

$$\Delta t \geq \frac{\Delta x^2}{6D} \quad (5.5)$$

That is, if the discretization parameters, Δt and Δx , satisfy inequality (5.5) then all the distributions f_i will be non-negative. Non-negativity of all f_i 's implies the non-negativity of the concentration $u(\mathbf{x}, t)$, which stems directly from equation (3.6).

Note that this result is only valid for one-dimensional pure diffusion equation (i.e., the advection velocity is zero) and for *D1Q3* lattice model. Furthermore, the above condition does not guarantee the preservation of the comparison principles. Deriving similar conditions for more sophisticated lattice models in two and three dimensions and for multiple-relaxation-time methods will require a more rigorous analysis.

Another noteworthy point is that we have put stronger conditions on the values of distributions f_i in order to meet the non-negative constraint for the concentration. In other words, for nodal concentrations to be non-negative we made sure that all the distributions are non-negative (i.e., $f_i(\mathbf{x}, t) \geq 0 \forall i$). However, this condition can be relaxed by allowing some of the f_i to be negative,

but with an additional constraint that $\sum_{i=0}^{m-1} f_i(\mathbf{x}, t) \geq 0$. We do not pursue such an approach here, but one can consider them in future developments of lattice Boltzmann methods.

6. DISCUSSION AND CONCLUDING REMARKS

The maximum and comparison principles are two important mathematical properties of diffusion-type equations. The non-negative constraint is an important physical constraint on the concentration in transport and reactive-transport equations. There are other properties that the solutions to diffusion-type equations satisfy under appropriate conditions on the input data; for example, the decay property. A main challenge in designing a predictive numerical formulation is to satisfy these mathematical principles and the physical constraints in the discrete setting. In this paper, using representative numerical examples, we have systematically documented that the current LBM-based formulations do not satisfy the maximum principle, the comparison principle, the non-negative constraint, and the decay property. We have also shown that the discretization of boundary conditions has an affect on the performance of the lattice Boltzmann method in meeting these properties. To this end, we proposed a new way of discretizing Dirichlet boundary conditions – the weighted splitting method. We then derived a theoretical bound in terms of the time-step and lattice cell size that guarantees non-negative values for the concentration under the weighted splitting method for one-dimension problems.

For anisotropic diffusion problems, we considered two representative multiple-relaxation-time lattice Boltzmann methods proposed in [Yoshida and Nagaoka, 2010] and [Huang and Wu, 2014]. We have shown that these multiple-relaxation-time methods can give unphysical negative values for the concentration. It needs to be emphasized that stability conditions for the lattice Boltzmann method (i.e., Courant-Fredrichs-Lewy conditions) have satisfied in all our numerical experiments. *This implies that meeting stability conditions alone does not guarantee the preservation of the mentioned mathematical principles in the discrete setting.* The main findings of the paper about LBM-based formulations can be summarized as follows:

- (a) **One-dimensional problems:** For a given time-step, one can eliminate the violation of the non-negative constraint and the maximum principle by refining the lattice cell size. For a given lattice cell size, the violation of the non-negative constraint and the maximum principle cannot be eliminated by decreasing the time-step. Both these trends are similar to the finite element method, which have been reported in [Nakshatrala et al., 2013b].
- (b) **Critical time-step:** Based on a simple theoretical analysis, we obtained the following bound for the time-step and lattice cell size to meet the non-negative constraint under LBM for 1D problems:

$$\Delta t \geq \frac{\Delta x^2}{6D} \tag{6.1}$$

One can obtain exactly the same bound under the single-field Galerkin finite element method based on the backward Euler time-stepping scheme for 1D problems [Nakshatrala et al., 2013b]. This is an interesting result given the fact that the underlying basis of the lattice Boltzmann method (which solves Boltzmann equation to obtain distributions at lattice nodes) is completely different from that of the finite element method (which is based on a weak formulation).

- (c) **Isotropic vs. anisotropic diffusion:** The violations of the non-negative constraint and the maximum principle are smaller in magnitude and smaller in terms of spatial extent when the diffusion is isotropic. Also, for a given time-step, one can decrease these violations by refining the lattice cell size in the case of isotropic diffusion. On the other hand, neither decreasing the time-step

nor refining the lattice cell size will eliminate the violation of the non-negative constraint for anisotropic diffusion.

- (d) **Convex vs. non-convex domains:** The magnitudes of the violation of the non-negative constraint are larger for non-convex domains. However, it needs to be emphasized that one may have violations even on convex domains.
- (e) **Comparison principle:** The lattice Boltzmann method violates the comparison principle even in a simple setting like 1D problems or isotropic diffusion. The violation of the comparison principle will be more predominant in the case of anisotropic diffusion.
- (f) **Decay property:** The LBM-based formulations, in general, violate the decay property.
- (g) The lattice Boltzmann method does not possess a variational structure, similar to the one proposed by the finite element method. Due to this reason, the non-negative formulations proposed under the finite element method (e.g., [Nakshatrala et al., 2013b]) cannot be directly extended to the lattice Boltzmann method.
- (h) The only procedure that is available to meet the non-negative constraint under the lattice Boltzmann method is the clipping procedure, which basically chops off the negative values. But, this procedure fixes neither the violation of the decay property nor the violation of the comparison principle. Moreover, this method does not have any physical or mathematical basis, and it is rather *ad hoc*.

One should be wary of violations of the non-negative constraint, and the maximum and comparison principles in the numerical simulations using LBM. In the case of *isotropic* diffusion, the authors suggest investigating the occurrence of the mentioned violations, if any of these violations occur, they can be significantly reduced by refining the lattice cell size and the time-step in accordance with the CFL condition. However, in the case of *anisotropic* diffusion, no clear-cut guideline for reducing the violations exists. As demonstrated earlier, refining the discretization parameters may not improve the numerical solution. A future research direction could be development of LBM-based formulations for transient diffusion-type equations (i.e., diffusion, advection-diffusion and advection-diffusion-reaction equations) that respect the maximum and comparison principles, and meet the non-negative constraint. This paper can serve as a source of benchmark problems for such a research endeavor.

ACKNOWLEDGMENTS

The authors acknowledge the support from the Department of Energy through Subsurface Biogeochemical Research Program. Neither the United States Government nor any agency thereof, nor any of their employees, makes any warranty, express or implied, or assumes any legal liability or responsibility for the accuracy, completeness, or usefulness of any information. The opinions expressed in this paper are those of the authors and do not necessarily reflect that of the sponsor(s).

References

- S. G. Ayodele, F. Varnik, and D. Raabe. Lattice Boltzmann study of pattern formation in reaction-diffusion systems. *Physical Review E*, 83:016702, 2011.
- Z. Chai and T. S. Zhao. Lattice Boltzmann model for convection-diffusion equation. *Physical Review E*, 87:63309, 2013.
- S. Chen and G. D. Doolen. Lattice Boltzmann methods for fluid flows. *Annual Review of Fluid Mechanics*, 30:329–364, 1998.

- L. C. Evans. *Partial Differential Equations*. American Mathematical Society, Providence, Rhode Island, 1998.
- G. Falcucci, S. Ubertini, C. Biscarini, S. Di Francesco, D. Chiappini, S. Palpacelli, A. De Maio, and S. Succi. Lattice Boltzmann methods for multiphase flow simulations across scales. *Communications in Computational Physics*, 1:1–35, 2006.
- X. He and L. Lou. Theory of the lattice Boltzmann method: From the Boltzmann equation to the lattice Boltzmann equation. *Physical Review E*, 56:6811, 1997.
- R. Huang and H. Wu. A modified multiple-relaxation-time lattice Boltzmann model for convection-diffusion equation. *Journal of Computational Physics*, 274:50–63, 2014.
- P. Lallemand and L. S. Lou. Theory of lattice Boltzmann method: Dispersion, dissipation, isotropy, Galilean invariance, and stability. *Physical Review E*, 61:6546, 2000.
- Q. Li, Y. L. He, G. H. Tang, and W. Q. Tao. Improved axisymmetric lattice Boltzmann scheme. *Physical Review E*, 81(5):056707, 2010.
- R. Liska and M. Shashkov. Enforcing the discrete maximum principle for linear finite element solutions for elliptic problems. *Communications in Computational Physics*, 3:852–877, 2008.
- K. B. Nakshatrala and A. J. Valocchi. Non-negative mixed finite element formulations for a tensorial diffusion equation. *Journal of Computational Physics*, 228:6726–6752, 2009.
- K. B. Nakshatrala, M. K. Mudunuru, and A. J. Valocchi. A numerical framework for diffusion-controlled bimolecular-reactive systems to enforce maximum principles and the non-negative constraint. *Journal of Computational Physics*, 253:278–307, 2013a.
- K. B. Nakshatrala, H. Nagarajan, and M. Shabouei. A numerical methodology for enforcing maximum principles and the non-negative constraint for transient diffusion equations. *arXiv:1206.0701*, 2013b.
- C. V. Pao. *Nonlinear Parabolic and Elliptic Equations*. Springer-Verlag, New York, USA, 1993.
- M. H. Protter and H. F. Weinberger. *Maximum Principles in Differential Equations*. Springer-Verlag, New York, 1999.
- A. F. Di Rienzo, P. Asinari, E. Chiavazzo, N. I. Prasianakis, and J. Mantzaras. Lattice Boltzmann model for reacting flow simulations. *Europhysics Letters*, 98:34001, 2012.
- B. Shi and Z. Guo. Lattice Boltzmann model for nonlinear convection-diffusion equations. *Physical Review E*, 79:16701, 2009.
- M. Stiebler, J. Tolke, and M. Krafczyk. Advection-diffusion lattice Boltzmann scheme for hierarchical grids. *Computers and Mathematics with Applications*, 55:1576–1584, 2008.
- S. Succi. *The Lattice Boltzmann Equation for Fluid Dynamics and Beyond*. Oxford University Press, Oxford, 2001.
- T. W. Willingham, C. J. Werth, and A. J. Valocchi. Evaluation of the effects of porous media structure on mixing-controlled reactions using pore-scale modeling and micromodel experiments. *Environmental Science & Technology*, 42:3185–3193, 2008.
- H. Yoshida and M. Nagaoka. Multiple-relaxation-time lattice Boltzmann model for the convection and anisotropic diffusion equation. *Journal of Computational Physics*, 229:7774–7795, 2010.

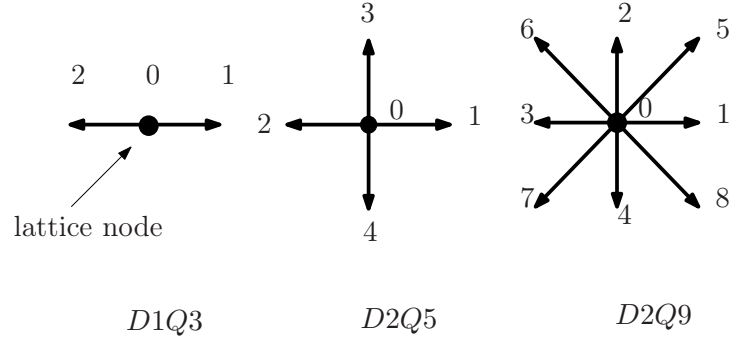


FIGURE 1. This figure shows the one- and two-dimensional lattice models that have been employed in this paper.

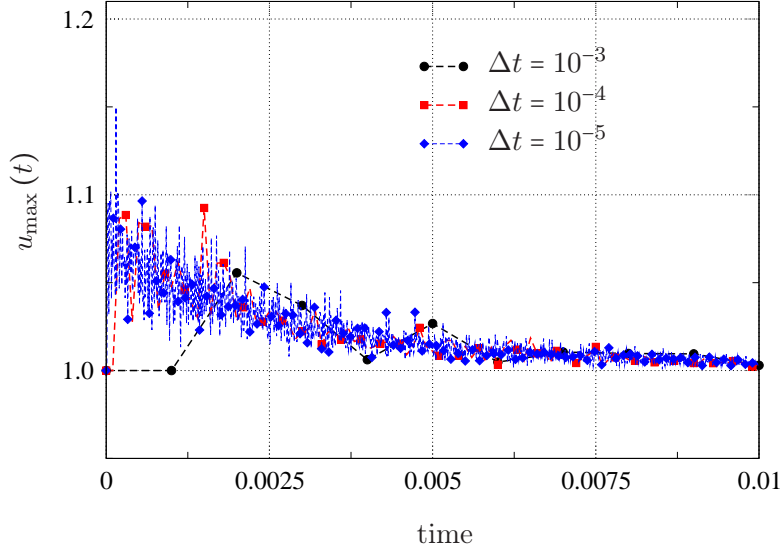


FIGURE 2. One-dimensional problem with uniform initial condition: The maximum nodal concentration is plotted against time for various time-steps. In all the cases, the lattice cell size is taken as $\Delta x = 0.1$. For the prescribed data, the maximum principle asserts that the concentration should be between 0 and 1 in the entire domain and for all times. *This figure shows that the single-relaxation-time method violates the maximum principle. Moreover, reducing the time-step keeping the lattice cell size fixed may not eliminate the violation of the maximum principle.*

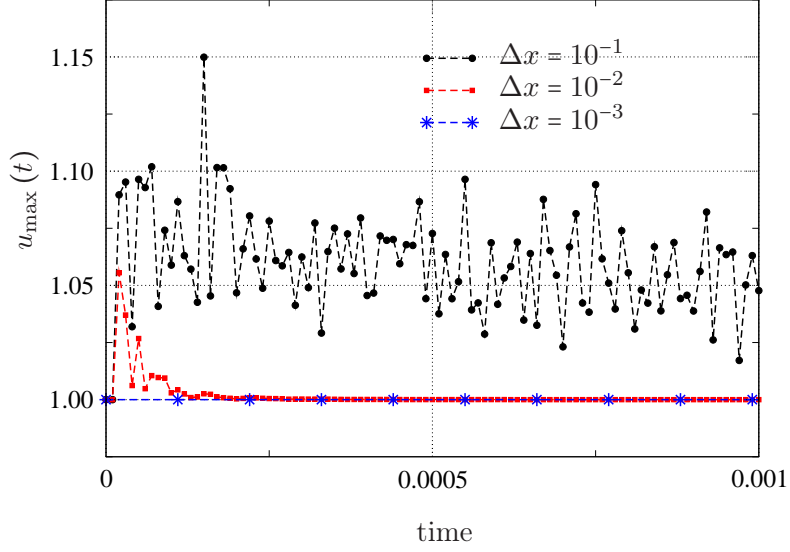


FIGURE 3. One-dimensional problem with uniform initial condition: The maximum nodal concentration is plotted against time for various lattice cell sizes. The time-step is arbitrarily chosen as $\Delta t = 10^{-5}$ for all cases. *It can be observed that, for a chosen time-step, reducing the lattice cell size can eliminate the violation of the maximum principle for one-dimensional problems.*

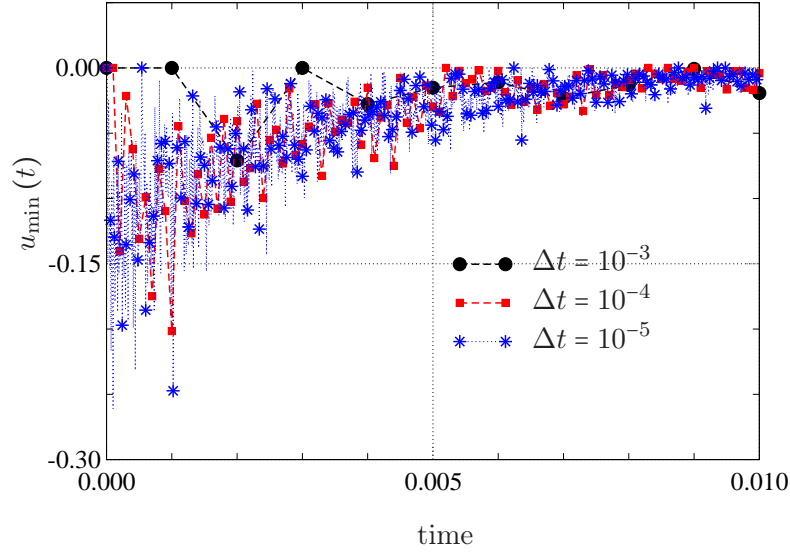
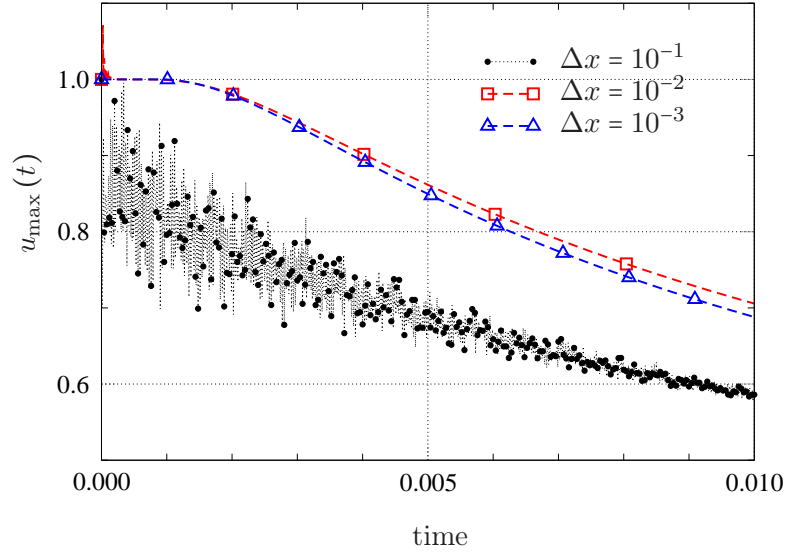
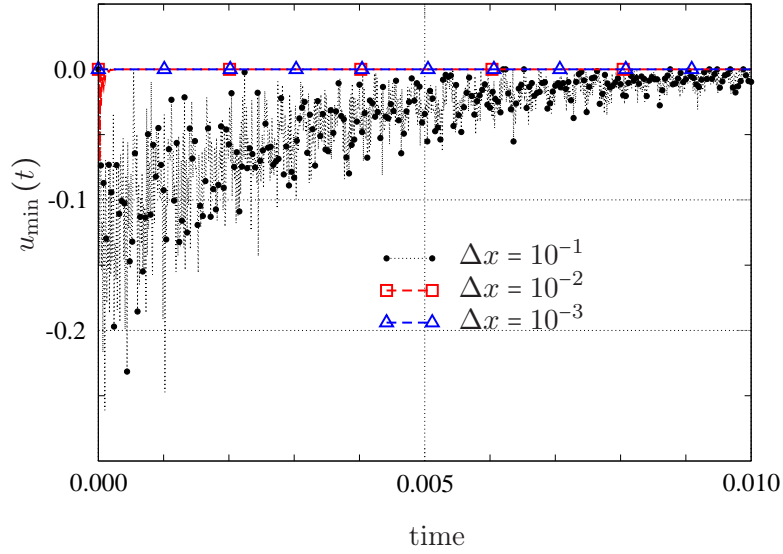


FIGURE 4. One-dimensional problem with non-uniform initial condition: The minimum nodal concentration is plotted against time for various time-steps. The lattice cell size is taken as $\Delta x = 0.1$. For the given input data, the maximum principle asserts that the concentration should be between 0 and 1 for all times. *The numerical solutions under the LBM have violated the non-negative constraint. It can be observed that reducing the time-step may not eliminate the violation of the non-negative constraint.*

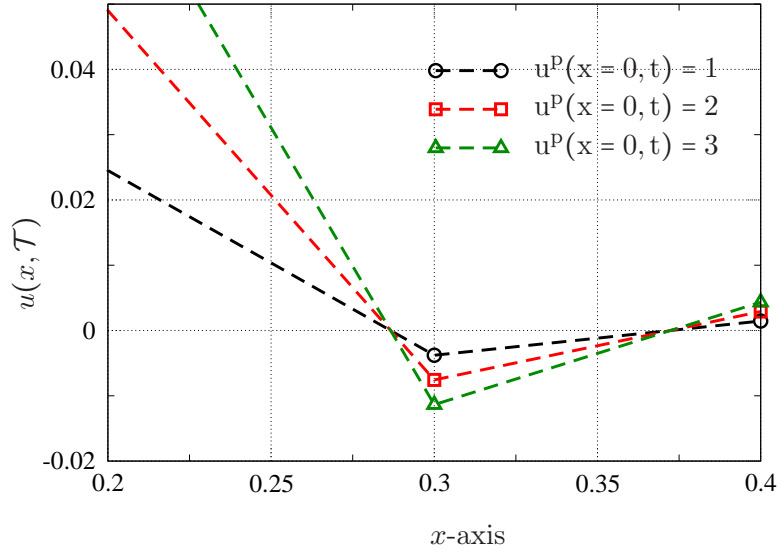


(a)

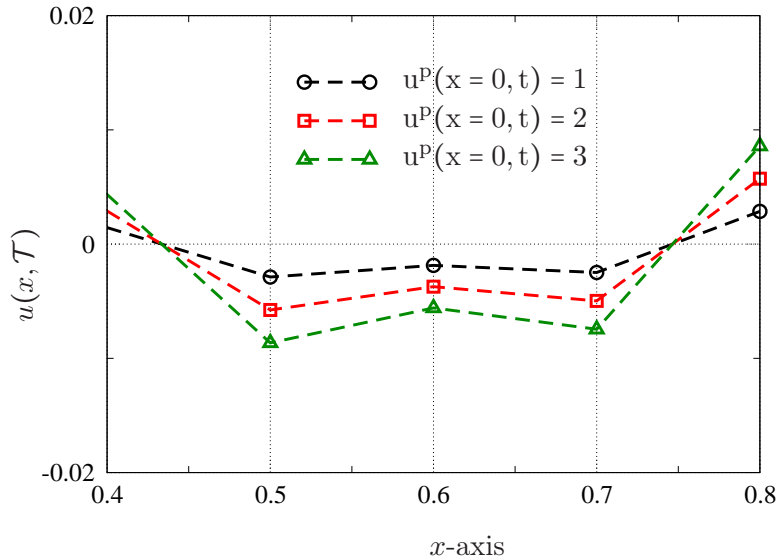


(b)

FIGURE 5. One-dimensional problem with non-uniform initial condition: Maximum and minimum nodal concentrations are plotted against the time for various lattice cell sizes. The lattice time-step is taken as $\Delta t = 10^{-5}$. The concentration should be between 0 and 1. The numerical solutions have clearly violated the maximum (see near $t = 0$) and minimum bounds. However, it is observed that, for a fixed time-step, reducing the lattice cell size Δx can decrease the violation.



(a) Violation of the comparison principle near $x = 0.3$.



(b) Violation of the comparison principle near $x = 0.5$ and $x = 0.7$.

FIGURE 6. One-dimensional problem and the comparison principle: The source is taken to be zero (i.e., $g(x, t) = 0$), and the initial concentration is zero in the entire domain. The lattice cell size is $\Delta x = 0.1$ and the time-step is $\Delta t = 10^{-5}$. The prescribed concentration at $x = 1$ is zero, and three different cases are considered for the prescribed concentration at $x = 1$, as indicated in the figure. *It can be observed that the LBM based on the D1Q3 lattice model violates the comparison principle.*

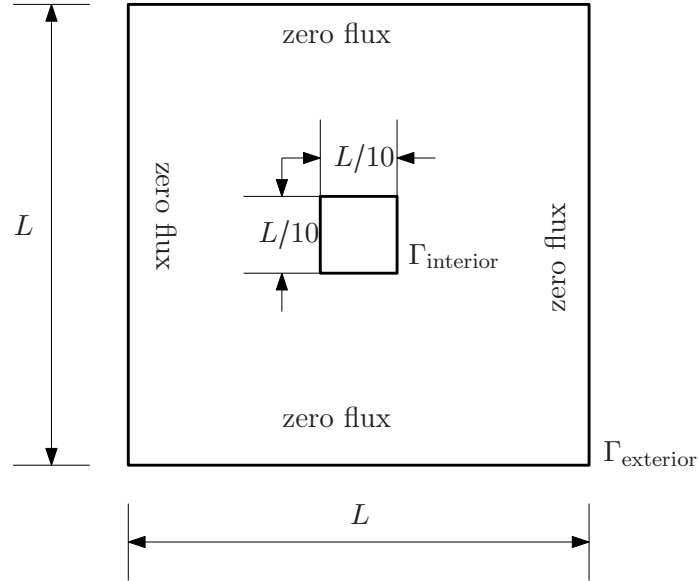


FIGURE 7. Two-dimensional problem with anisotropic diffusion in a non-convex domain: This figure provides a pictorial description of the test problem. A concentration of $u^P = 1$ is prescribed on the inner boundary.

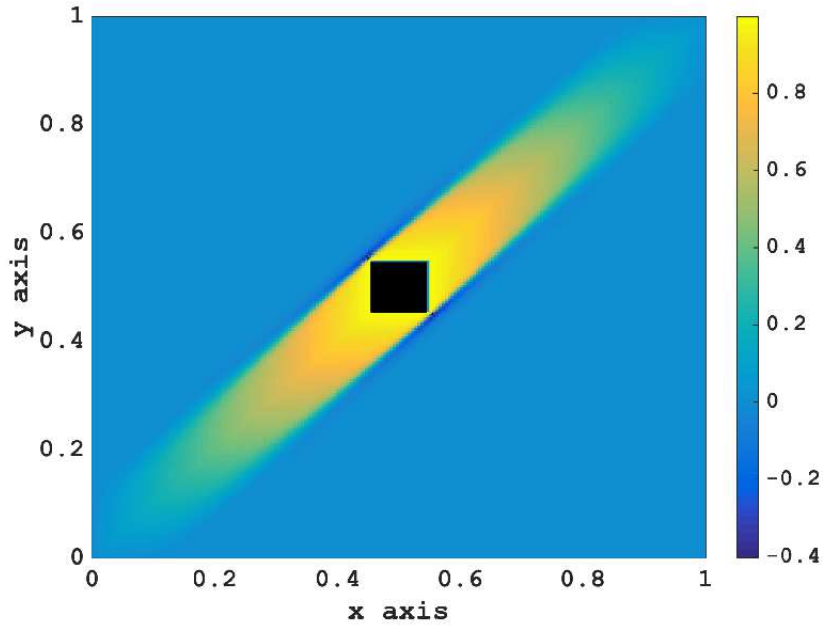
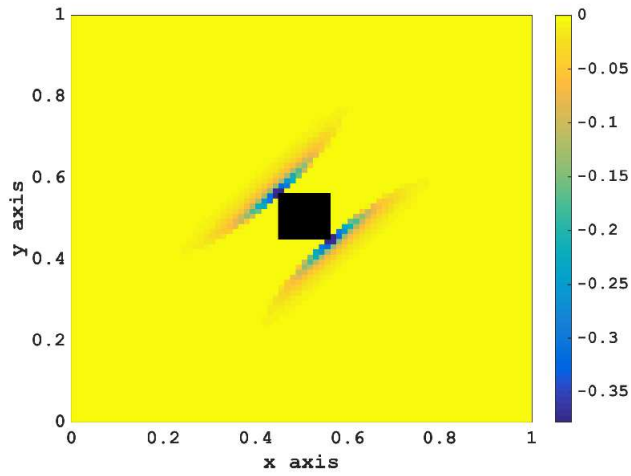
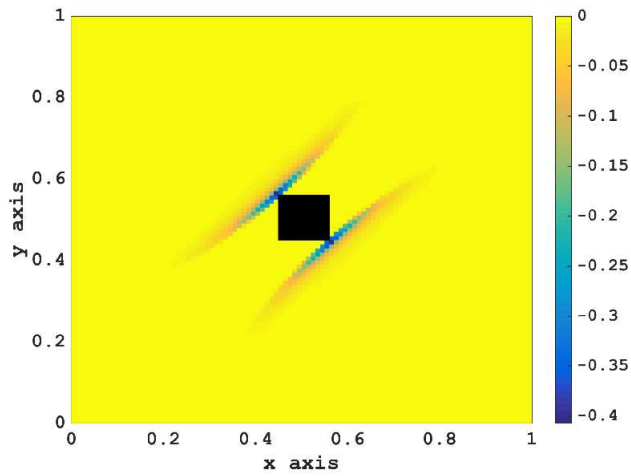


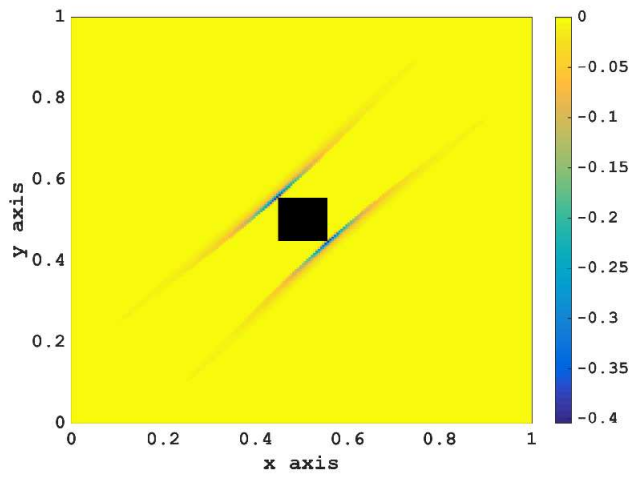
FIGURE 8. Two-dimensional problem with anisotropic diffusion in a non-convex domain: This figure shows the concentration profile at time $t = 0.01$ under the Y-N method for the data given by Case 3 in Table 2. The diffusivity tensor is anisotropic but spatially homogeneous. *Significant negative values for the concentration are observed in the computational domain.*



(a) Case 1



(b) Case 2



(c) Case 3

FIGURE 9. Two-dimensional problem with β^2 anisotropic diffusion in a non-convex domain: The figure shows the regions where the non-negative constraint is violated under the Y-N method.

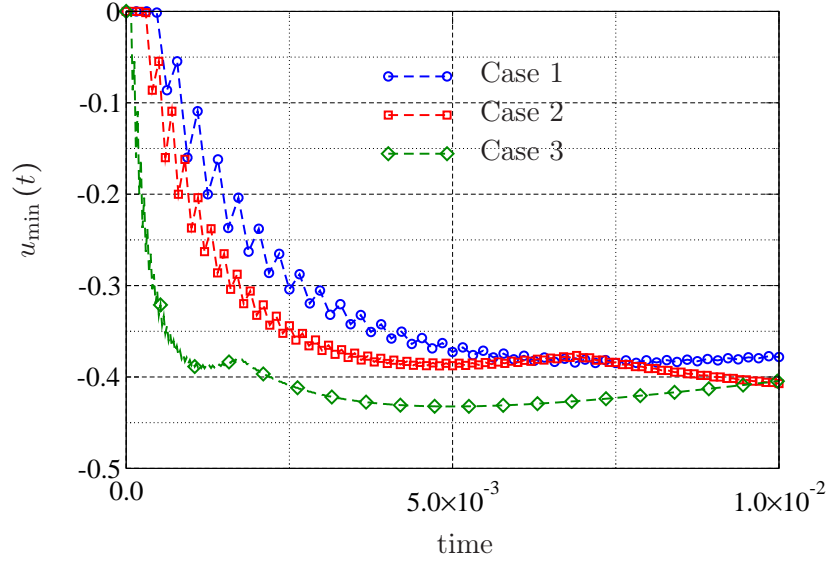


FIGURE 10. Two-dimensional problem with anisotropic diffusion in a non-convex domain: The figure shows the variation of minimum value of the concentration with respect to time under the Y-N multiple-relaxation-time lattice Boltzmann method. *It is evident from this numerical experiment that refining the discretization parameters, Δt and Δx , does not alleviate the violation of the non-negative constraint in the case of anisotropic diffusion.*

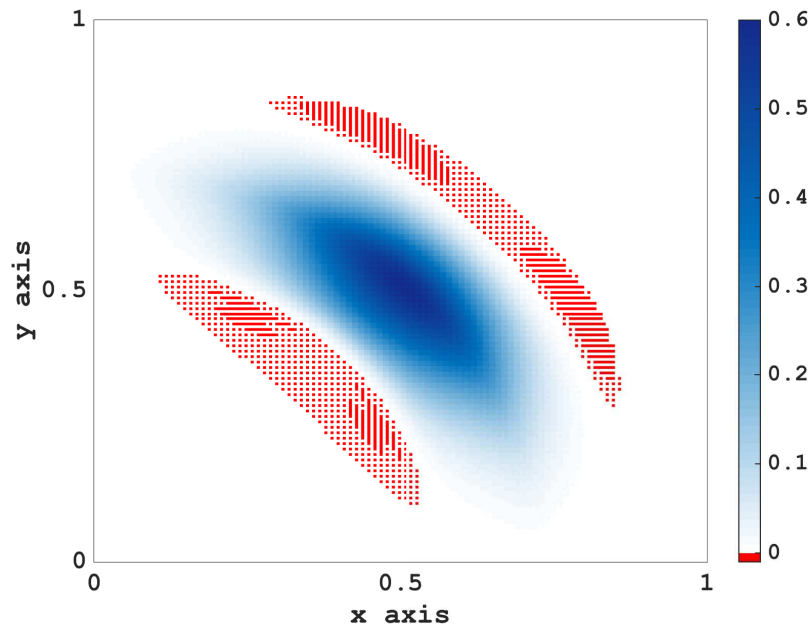


FIGURE 11. Two-dimensional problem with anisotropic and heterogeneous diffusion tensor: This figure shows the concentration profile at $t = 0.025$ under the H-W method. The parameters for this numerical experiment are given by Case 5 of Table 3. The minimum value of u is negative with $u_{\min}(\mathcal{T}) = -6.8 \times 10^{-3}$. (See the red regions on the online color version of this paper.)

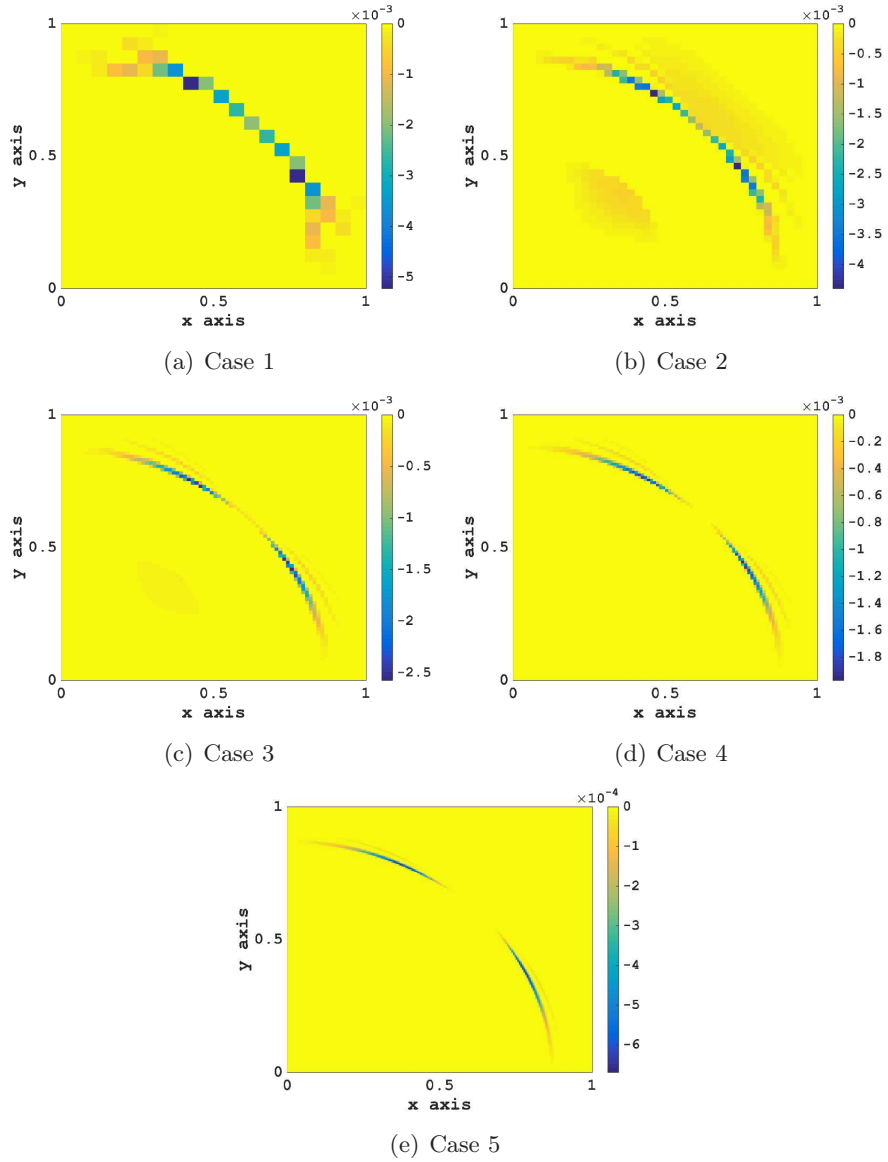
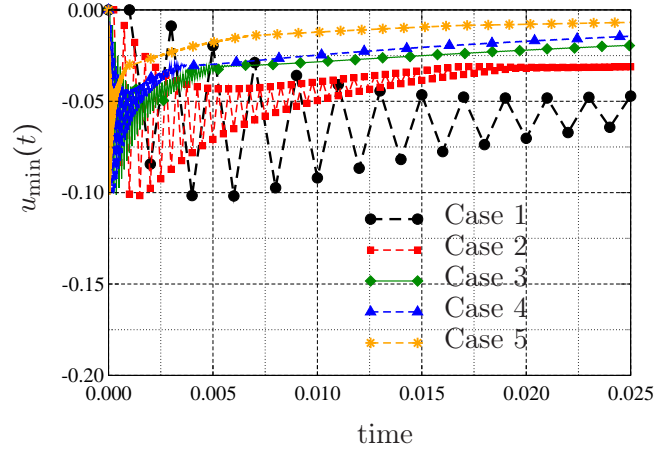
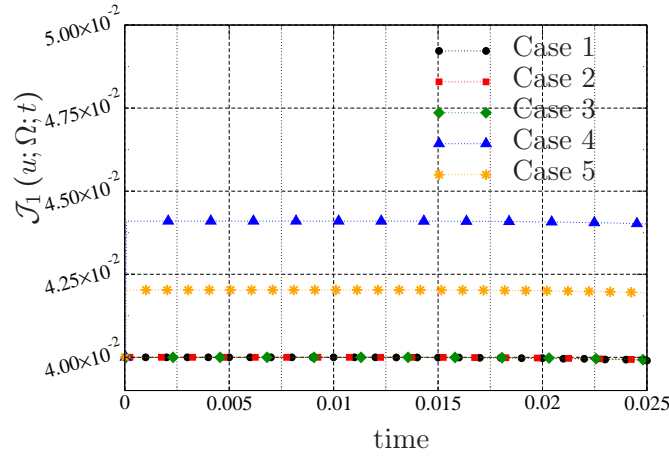


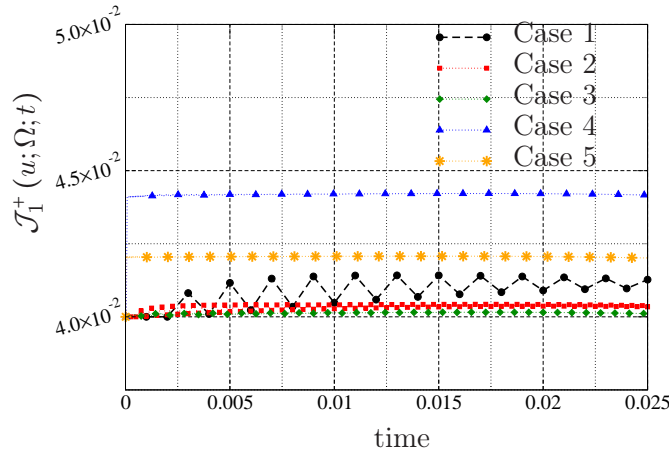
FIGURE 12. Two-dimensional problem with anisotropic and heterogeneous diffusion tensor: This figure shows the regions that have negative values for the concentration under the H-W method.



(a) Minimum nodal concentration.

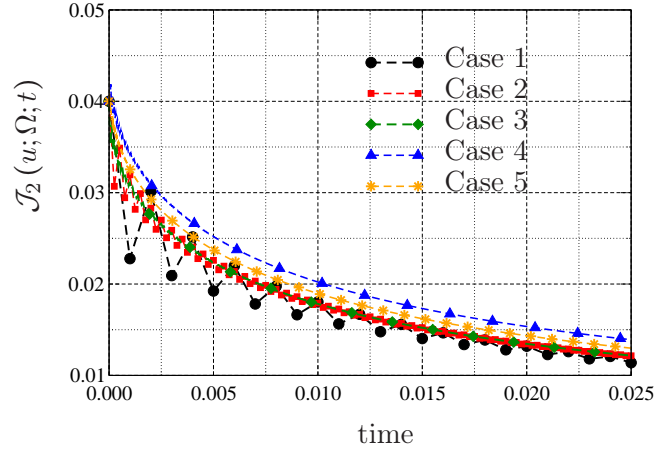


(b) Total amount of the dispersing chemical species with the negative values.

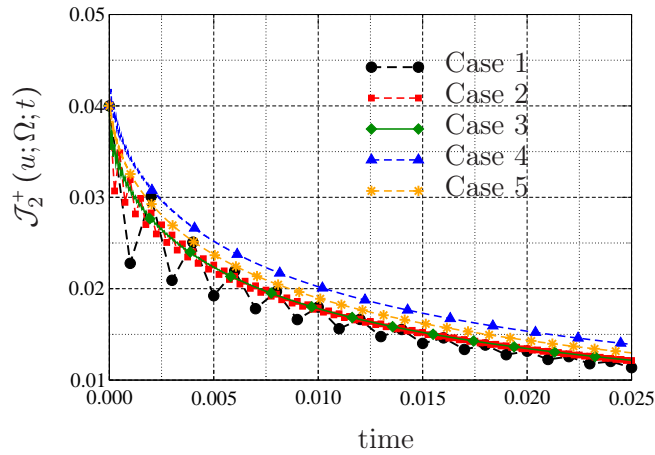


(c) Total amount of the dispersing chemical species *without* the negative values.

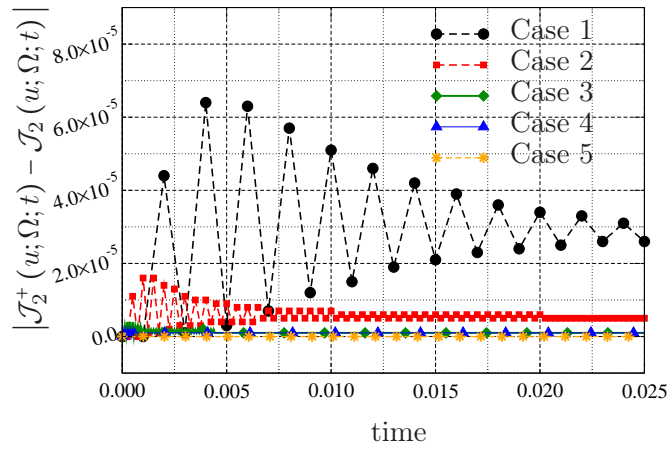
FIGURE 13. Two-dimensional problem with anisotropic and heterogeneous diffusion tensor: The total amounts of the diffusing species under the single-relaxation-time LBM and the clipping procedure are plotted against time. The variation of the minimum concentration over time is shown in the bottom figure. The parameters in various cases are provided in Table 3.



(a) Negative values are *not* clipped.



(b) Negative values are clipped.



(c) Resulting difference from clipping the negative values.

FIGURE 14. Two-dimensional problem with anisotropic and heterogeneous diffusion tensor: This figure shows the variation of various integrals defined in equation (2.10) with respect to time under the H-W method. The simulation parameters are provided in Table 3. *It is evident from the figure that the H-W method violated the decay property.*

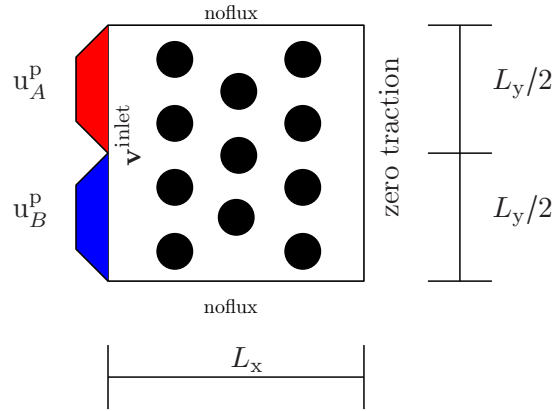


FIGURE 15. Fast bimolecular reaction in a porous medium: This figure provides a pictorial description of the test problem. We have taken $L_x = 1/2$ and $L_y = 2$ in the numerical experiment.

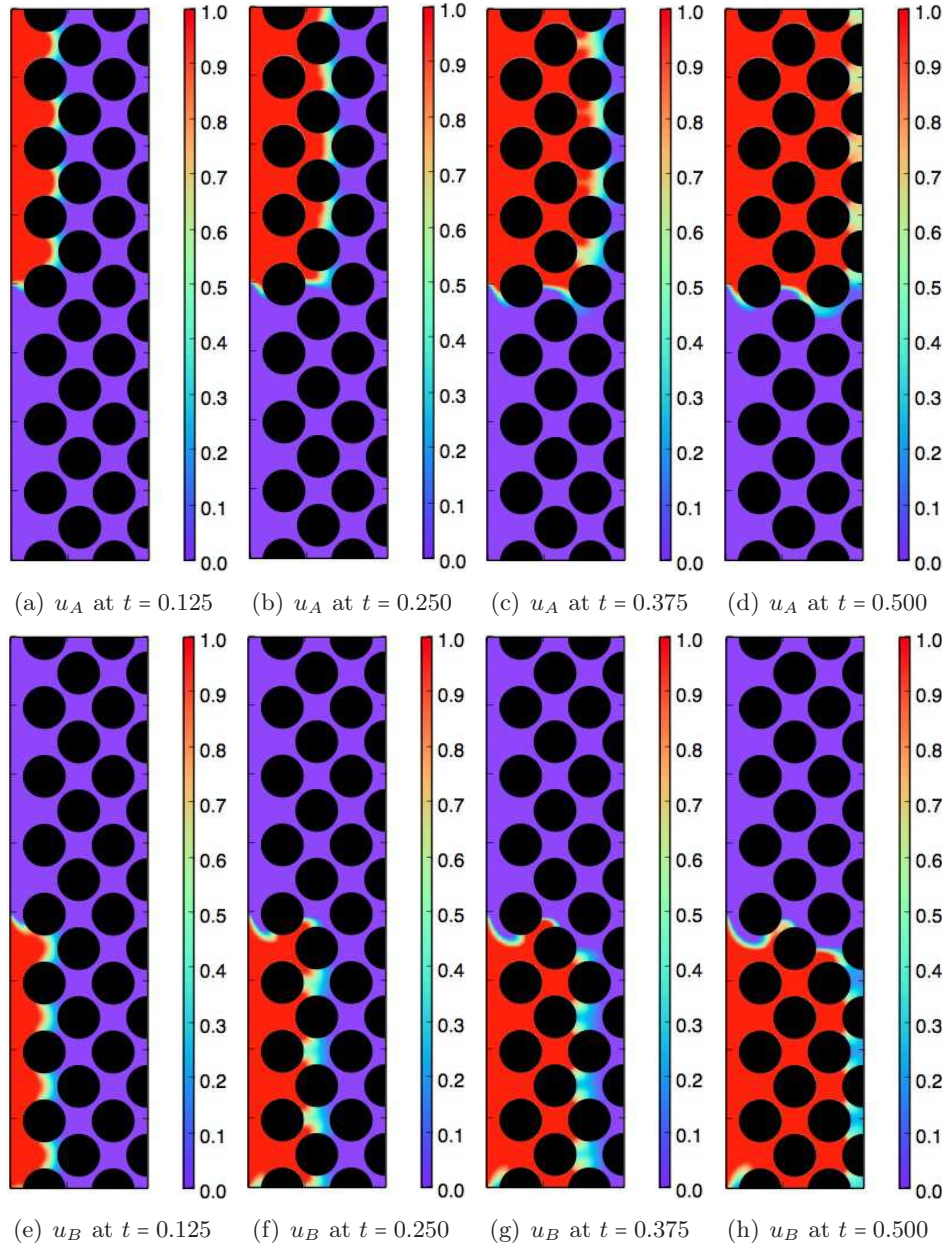


FIGURE 16. Fast bimolecular reaction in a porous medium: This figure shows the concentration profiles of the reactants A and B under the single-reaction-time method using the $D2Q9$ lattice model. The diffusivity tensor is isotropic, and no negative values for the concentration are observed for the reactants.

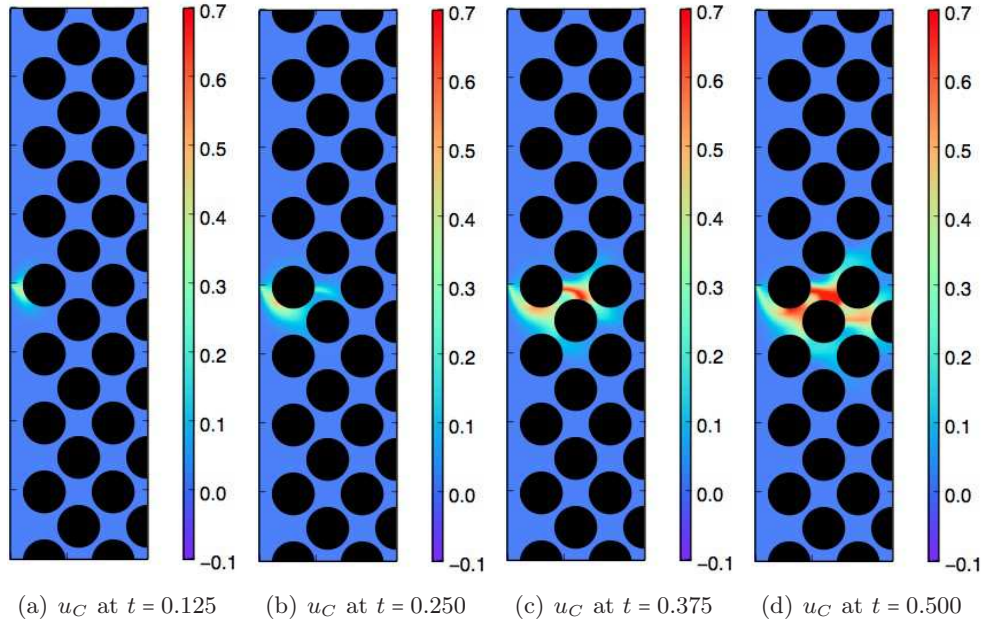


FIGURE 17. Fast bimolecular reaction in a porous medium: This figure shows the concentration profiles of the product C .

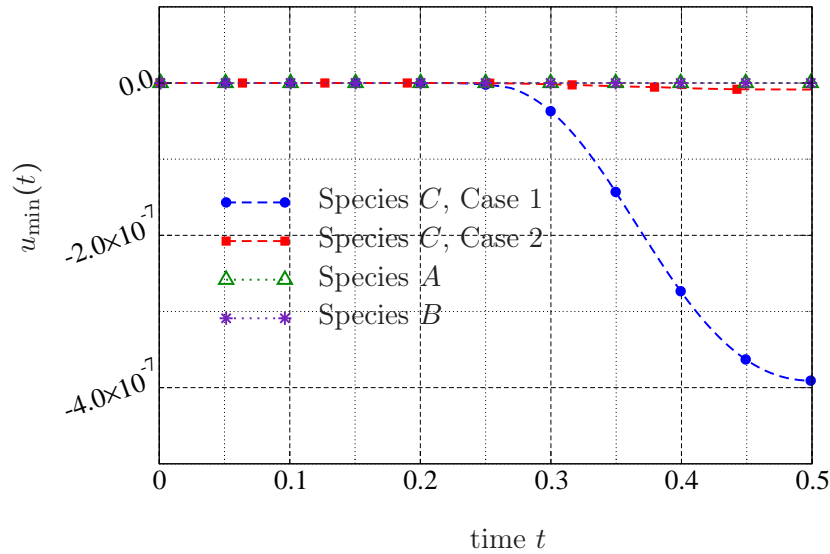


FIGURE 18. Fast bimolecular reaction in a porous medium: This figure shows the minimum observed values of the participating chemical species. Concentrations of the chemical species A and B did not violate the non-negative constraint. However, small negative concentration of the product C are observed. These violations did not diminish with time. But, the magnitude of the violation can be decreased by refining the discretization parameters.

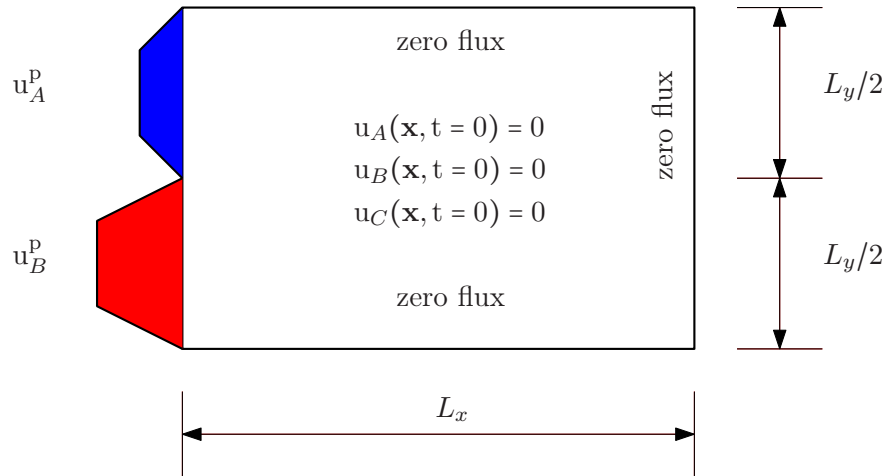


FIGURE 19. Fast bimolecular reaction in anisotropic and heterogeneous medium: This figure provides a pictorial description of the test problem. The reactants A and B undergo transport (i.e., both advection and diffusion) and reacts to give product C , which in turn gets transported. We have taken $L_x = 2$ and $L_y = 1$ in the numerical experiment.

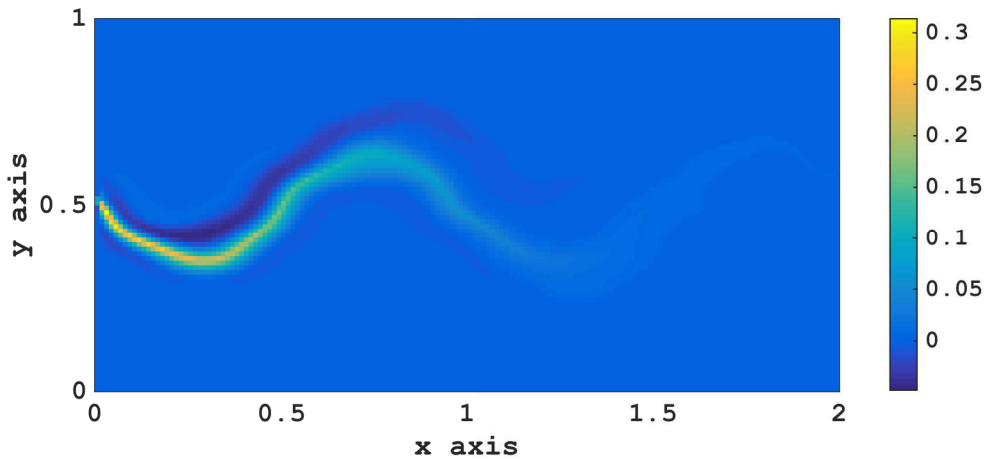
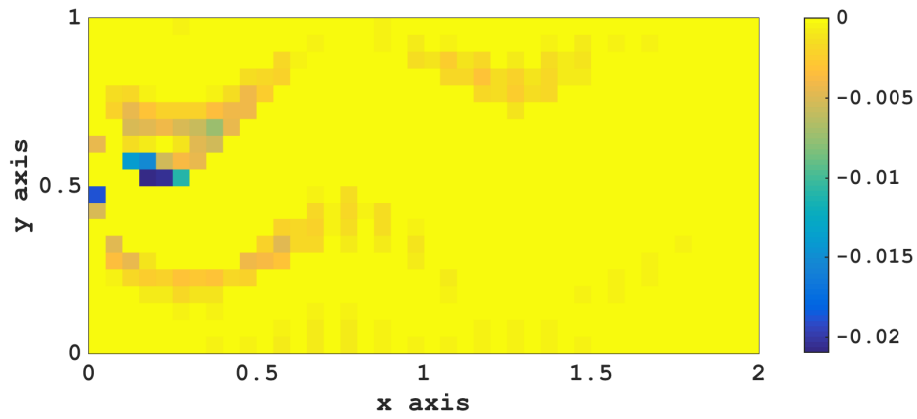
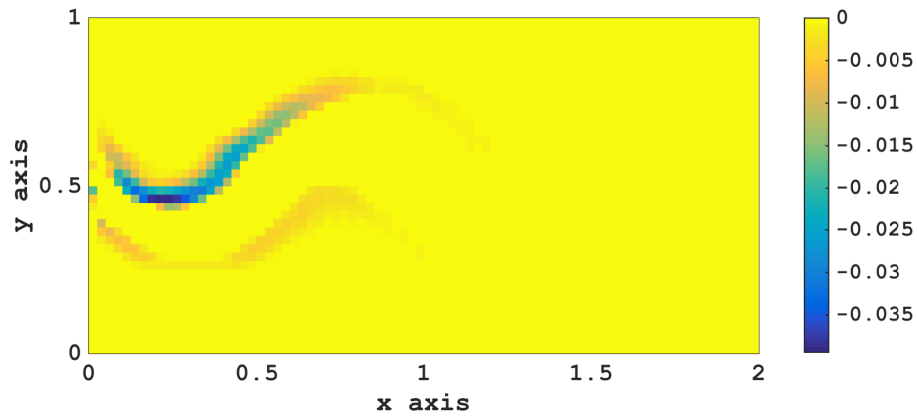


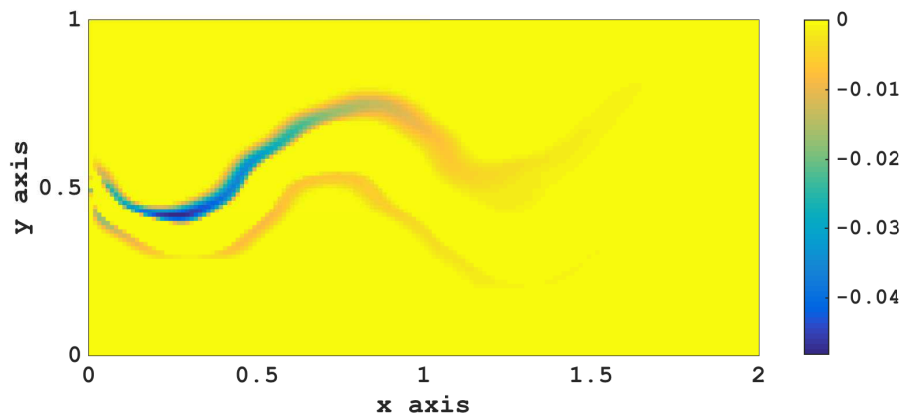
FIGURE 20. Fast bimolecular reaction in anisotropic and heterogeneous medium: This figure shows the concentration profile of the product C at $t = \mathcal{T} = 0.25$ under the H-W method. We have taken $\Delta x = 1.25 \times 10^{-2}$ and $\Delta t = 1.56 \times 10^{-6}$ (see Case 3 in Table 5).



(a) Case 1



(b) Case 2



(c) Case 3

FIGURE 21. Fast bimolecular reaction in anisotropic and heterogeneous medium: This figure shows the regions where the concentration of the product C is negative at $t = 0.25$ under the H-W method. The violations appear at large number of lattice nodes, and are spread across the computational domain.

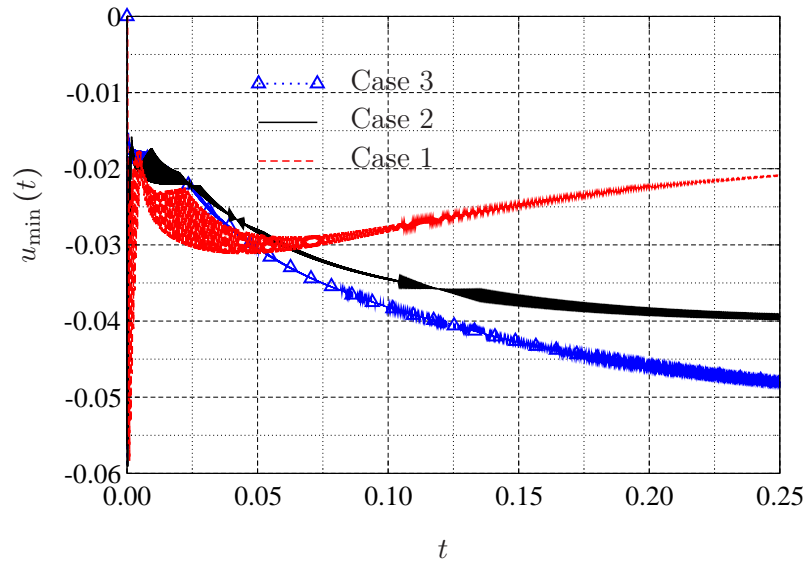


FIGURE 22. Fast bimolecular reaction in anisotropic and heterogeneous medium: The minimum concentration of the product C is plotted against time for various cases whose simulation parameters are provided in Table 4. *This figure clearly illustrates that refining the discretization parameters does not eliminate the violation of the non-negative constraint under the H-W method.*